Dysbiosis in imiquimod-induced psoriasis alters gut immunity and exacerbates colitis development

Gabriela Veronica Pinget, Jian Kai Tan, Duan Ni, Jemma Taitz, Claire Immediato Daien, Julie Mielle, Robert John Moore, Dragana Stanley, Stephen Simpson, Nicholas Jonathan Cole King, et al.

▶ **To cite this version:**

Gabriela Veronica Pinget, Jian Kai Tan, Duan Ni, Jemma Taitz, Claire Immediato Daien, et al.. Dysbiosis in imiquimod-induced psoriasis alters gut immunity and exacerbates colitis development. Cell Reports, 2022, 40 (7), pp.111191. 10.1016/j.celrep.2022.111191 . hal-03753669

HAL Id: hal-03753669
https://hal.science/hal-03753669v1

Submitted on 18 Aug 2022

HAL is a multi-disciplinary open access archive for the deposit and dissemination of scientific research documents, whether they are published or not. The documents may come from teaching and research institutions in France or abroad, or from public or private research centers.

L'archive ouverte pluridisciplinaire **HAL**, est destinée au dépôt et à la diffusion de documents scientifiques de niveau recherche, publiés ou non, émanant des établissements d'enseignement et de recherche français ou étrangers, des laboratoires publics ou privés.

Distributed under a Creative Commons Attribution - NonCommercial - NoDerivatives 4.0 International License

Dysbiosis in imiquimod-induced psoriasis alters gut immunity and exacerbates colitis development

Gabriela Veronica Pinget,[1,2,8] Jian Kai Tan,[1,2,8] Duan Ni,[1,2] Jemma Taitz,[1,2] Claire Immediato Daien,[1,3] Julie Mielle,[1,3] Robert John Moore,[4] Dragana Stanley,[5] Stephen Simpson,[1,6] Nicholas Jonathan Cole King,[1,2] and Laurence Macia[1,2,7,9,*]

[1]The Charles Perkins Centre, The University of Sydney, Sydney, NSW 2006, Australia
[2]School of Medical Sciences, Chronic Diseases Theme, Faculty of Medicine and Health, The University of Sydney, Sydney, NSW 2006, Australia
[3]CHRU Montpellier, University of Montpellier & INSERM U1046, CNRS UMR, PhyMedExp, 9214 Montpellier, France
[4]School of Science, RMIT University, Bundoora, VIC 3083, Australia
[5]School of Health, Medical and Applied Sciences, Central Queensland University, Kawana, QLD 4701, Australia
[6]School of Life and Environmental Sciences, Faculty of Sciences, The University of Sydney, Sydney, NSW 2006, Australia
[7]Sydney Cytometry, The University of Sydney, Sydney, NSW 2006, Australia
[8]These authors contributed equally
[9]Lead contact
*Correspondence: laurence.macia@sydney.edu.au
https://doi.org/10.1016/j.celrep.2022.111191

SUMMARY

Psoriasis has long been associated with inflammatory bowel disease (IBD); however, a causal link is yet to be established. Here, we demonstrate that imiquimod-induced psoriasis (IMQ-pso) in mice disrupts gut homeostasis, characterized by increased proportions of colonic $CX_3CR_1^{hi}$ macrophages, altered cytokine production, and bacterial dysbiosis. Gut microbiota from these mice produce higher levels of succinate, which induce *de novo* proliferation of $CX_3CR_1^{hi}$ macrophages *ex vivo*, while disrupted gut homeostasis primes IMQ-pso mice for more severe colitis with dextran sulfate sodium (DSS) challenge. These results demonstrate that changes in the gut environment in psoriasis lead to greater susceptibility to IBD in mice, suggesting a two-hit requirement, that is, psoriasis-induced altered gut homeostasis and a secondary environmental challenge. This may explain the increased prevalence of IBD in patients with psoriasis.

INTRODUCTION

Psoriasis is a chronic autoinflammatory skin disorder that is estimated to affect 2%–4% of the world's population (Christophers, 2001; Chandran and Raychaudhuri, 2010; Parisi et al., 2013). Plaque psoriasis, which accounts for 90% of cases, is characterized by red, scaly plaques; epidermal hyperplasia; accumulation of inflammatory cells in the dermis; and activation of interleukin (IL)-23- and IL-17-producing cells, similar to the imiquimod-induced mouse model of psoriasis (IMQ-pso) (Di Cesare, Di Meglio and Nestle, 2009; Cai et al., 2011; Dogra and Mahajan, 2016).

Psoriasis is associated with several comorbidities, including metabolic syndrome, obesity, non-alcoholic fatty liver disease, and cardiovascular diseases (Neimann et al., 2006; Kimball et al., 2008; van der Voort et al., 2014; Balato et al., 2015; Dogra and Mahajan, 2016). Notably, people with psoriasis are also more likely to exhibit disrupted intestinal barrier integrity and altered gut microbiota (dysbiosis) and are seven times more likely to suffer from inflammatory bowel disease (IBD) than the general population (Christophers, 2001; Li et al., 2013; de Oliveira et al., 2015; Codoner et al., 2018; Sikora et al., 2018; Tan et al., 2018; Visser et al., 2019). However, the mechanisms underlying this are unknown. The functional role of gut microbiota in psoriasis has been established, with neonatal mice treated with antibiotics developing exacerbated disease, while probiotic administration reduced psoriasis-associated inflammation in patients (Groeger et al., 2013) and reduced psoriatic skin lesions in mice (Chen et al., 2017b).

The gut microbiota affects the host through various mechanisms, particularly via the production of metabolites, such as short-chain fatty acids (SCFAs) (Tan et al., 2014; Morita et al., 2019). These metabolites regulate the expansion of colonic immune cells and can alter their cytokine profile to regulate the gut inflammatory environment (Furusawa et al., 2014; Nastasi et al., 2015; Tan et al., 2016; Bhaskaran et al., 2018; Morita et al., 2019). While SCFAs have anti-inflammatory effects, other metabolites, such as succinate, shown to be elevated in IBD patients (Connors et al., 2018), can have pro-inflammatory effects and act to increase macrophage activation (Fremder et al., 2021). Thus, changes in gut microbiota and associated metabolites may contribute to IBD development.

Macrophages make up 20% of colonic leukocytes and are a key immune subset involved in gut homeostasis. They orchestrate inflammatory and repair processes within the colon via the production of chemokines and cytokines, to recruit and

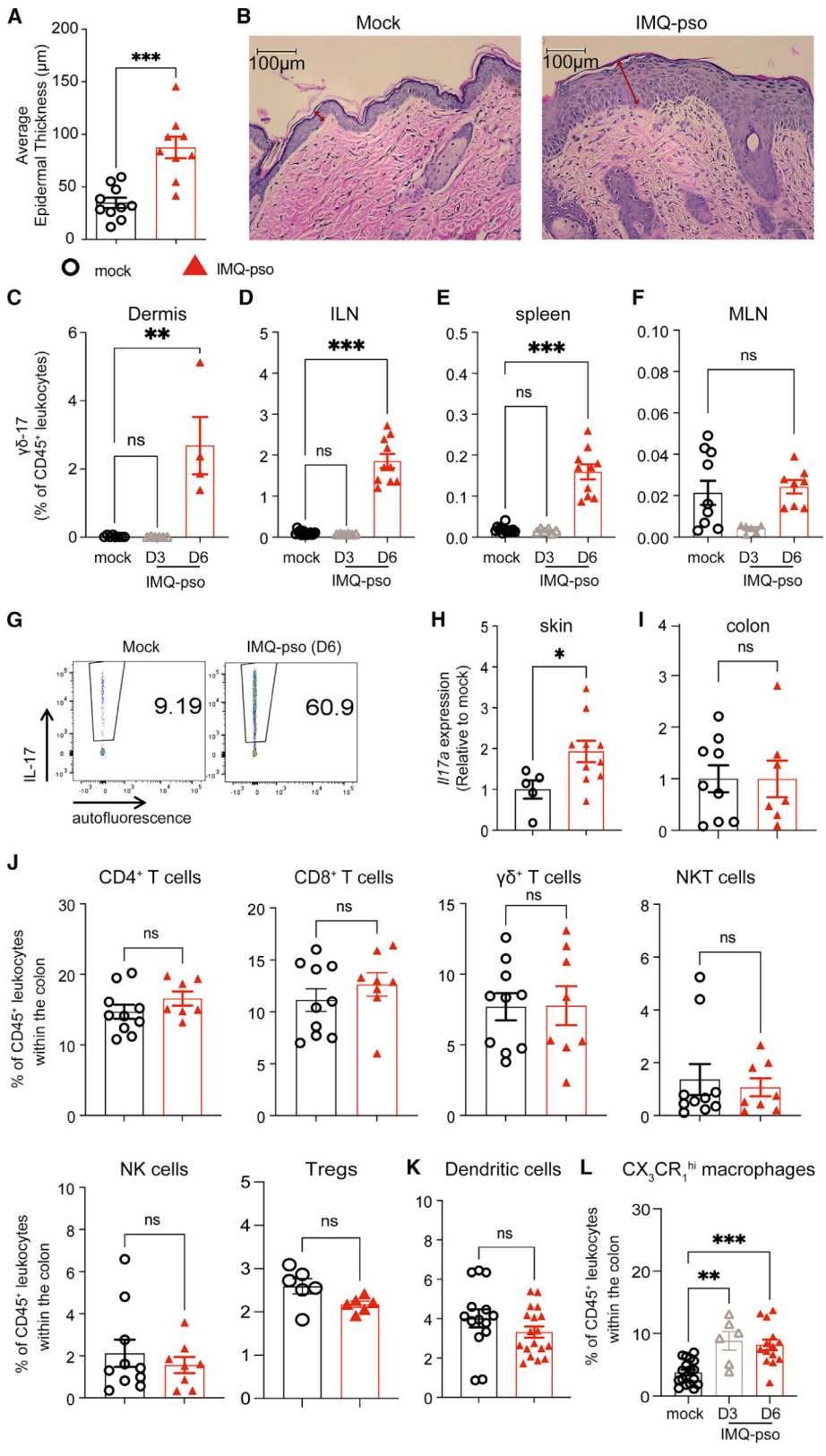
A
Average Epidermal Thickness (μm)
200
150
100
50
0
***
mock
IMQ-pso
B
Mock
IMQ-pso
100μm
100μm
C
Dermis
γδ-17 (% of CD45⁺ leukocytes)
**
ns
mock
D3
D6
IMQ-pso
D
ILN
***
ns
E
spleen
***
ns
F
MLN
ns
G
Mock
IMQ-pso (D6)
9.19
60.9
IL-17
autofluorescence
H
skin
Il17a expression (Relative to mock)
*
I
colon
ns
J
CD4⁺ T cells
CD8⁺ T cells
γδ⁺ T cells
NKT cells
% of CD45⁺ leukocytes within the colon
NK cells
Tregs
K
Dendritic cells
L
CX3CR1hi macrophages
***
**

maintain effector immune cells (Medina-Contreras et al., 2011; Bain and Schridde, 2018; Schulthess et al., 2019). Impaired macrophage function promotes the development of IBD (Han et al., 2021), and these cells are thus often the target of novel IBD therapies (Steinbach and Plevy, 2014; Na et al., 2019). However, whether psoriasis affects gut immunity, in particular, colonic macrophage activity, is unknown.

Currently, a critical knowledge gap exists with respect to psoriasis and the associated changes in gut homeostasis to explain why patients with psoriasis are more likely to develop IBD. Using the IMQ-pso mouse model, we show that psoriasis alters the gut microbiota composition and promotes the expansion of colonic $CX_3CR_1^{hi}$ macrophages. A psoriasis-associated microbiota is geared toward a greater capacity for succinate production, which directly contributes to the higher *in situ* proliferation of colonic $CX_3CR_1^{hi}$ macrophages. This disrupted psoriasis gut homeostasis contributes to exacerbated dextran sulfate sodium (DSS)-induced colitis, providing a causal link between psoriasis and IBD.

RESULTS

Imiquimod-induced psoriasis specifically increased $CX_3CR_1^{hi}$ macrophages in the colon

Like human psoriasis, IMQ-pso is characterized by systemic as well as dermal immune changes (Grine et al., 2016). However, whether immune changes specifically within the colon and gut-draining lymph nodes occur during IMQ-pso remains unknown. To address this question, we induced psoriasis in mice through topical application of IMQ on the upper dorsal skin and assessed the immune cell profile by flow cytometry in the skin, inguinal lymph nodes, spleen, mesenteric lymph nodes, and colon. As previously reported (van der Fits et al., 2009), IMQ-pso resulted in epidermal thickening (as indicated by red arrows; Figures 1A and 1B), skin thickening, scaling, and erythema (Figure S1A), as well as splenomegaly (Figure S1B). The inflammatory process in IMQ-pso is largely driven by the cytokine IL-17, produced primarily by $\delta\gamma$ T cells (Cai et al., 2011), which we found to be increased by day 6 in the affected dermis (Figure 1C), the skin-draining inguinal lymph nodes (ILNs) (Figure 1D) (representative plots shown in Figure 1G), and the spleen (Figure 1E), but not in the gut-draining mesenteric lymph nodes (MLNs) (Figure 1F). These findings were also reflected in the total cell count (Figure S1C). Consistent with these flow cytometry results, IL-17A mRNA expression was increased in the affected skin (Figure 1H) (drained by ILN) but not in the colon (drained by MLN) of IMQ-pso mice (Figure 1I). A deeper investigation of the immune status in the colon of IMQ-pso mice shows no alteration in the proportions of lymphoid cells, including $CD4^+$ T, regulatory T, $CD8^+$ T, $\gamma\delta$ T, and natural killer T cells and natural killer cells (Figure 1J; gating strategy Figure S2A), or in the myeloid compartment, particularly dendritic cells (Figure 1K). Deeper analysis of the ILN, spleen, and MLN revealed changes consistent with the IMQ-pso disease model, particularly increased $\gamma\delta$ T cell populations in the ILN and spleen (Figure S2B). However, we found a significant increase in the proportion of $CX_3CR_1^{hi}$ macrophages at days 3 and 6 at this site (Figure 1L; gating strategy Figure S2C), as well as increased numbers (Figure S2C). These data imply that psoriasis-associated inflammation has an impact on colonic immunity, specifically on $CX_3CR_1^{hi}$ macrophages, but not on other immune subsets.

The increase in colonic $CX_3CR_1^{hi}$ macrophages in psoriasis is due to *in situ* macrophage proliferation and not to monocyte infiltration

Colonic resident CX_3CR1^{hi} macrophages are of embryonic origin and are maintained *in situ* or replenished by blood-derived $Ly6C^{hi}$ monocytes (Bain et al., 2012; Shaw et al., 2018; Cossarizza et al., 2019; Desalegn and Pabst, 2019). To determine whether the rise in colonic CX_3CR1^{hi} macrophages observed in IMQ-pso was linked to monocyte infiltration, we injected mice intravenously with immune modifying particles (IMPs). These inert, negatively charged particles are taken up by $Ly6C^{hi}$ monocytes, which, as a result, become sequestered in the spleen, thereby preventing them from migrating to sites of inflammation (Getts et al., 2014; Pinget et al., 2020). Mice were treated daily with either 4.26×10^9 IMPs dispersed in saline or saline alone from the first day of IMQ treatment. As previously demonstrated, the numbers of $Ly6C^{hi}$ monocytes were significantly higher in the spleen of IMP-treated mice (data presented in Figures 4A and 4B in Pinget et al., 2020). However, despite IMP treatment, the proportion of $CX_3CR_1^{hi}$ macrophages in the IMQ-pso group remained similar to that of the saline-treated controls and significantly higher than that of the

Figure 1. IMQ-pso leads to increased $CX_3CR_1^{hi}$ macrophages in the colon of mice

Mice were either untreated (mock) or treated daily with 2 mg imiquimod (IMQ-pso) on the dorsal shaved skin.

(A and B) Epidermal thickness (μm) was measured on H&E-stained skin sections from these mice at day 6 (A) using the ImageJ software. Representative H&E-stained skin sections are shown (B) (n = 10 biological replicates/group). Red arrows, epidermal thickening.

(C–G) Proportions of $\gamma\delta$ IL-17^+ T cells among total leukocytes ($CD45^+$ cells) were determined by flow cytometry in mice treated daily for 0, 3, and 6 days with 2 mg imiquimod after stimulation of cells isolated from the dermis (C), inguinal lymph node (ILN) (D), spleen (E), and mesenteric lymph node (MLN) (F) for 4 h with phorbol 12-myristate 13-acetate (PMA) (10 ng/mL), ionomycin (1 μg/mL), and brefeldin A (5 μg/mL) *ex vivo*. Representative flow cytometry plots of ILN $\gamma\delta$ IL-17^+ T cells in mock (left) and IMQ-pso mice (right) (G) (n = 4–10 biological replicates/group).

(H and I) IL-17A expression by qPCR in the skin (H) and colon (I) of mock and IMQ-pso mice at day 6, represented as a fold change relative to average mock expression (n = 4–10 biological replicates/group).

(J and K) Proportions of colonic lamina propria $CD4^+$, $CD8^+$, $\gamma\delta^+$, natural killer T (NKT), natural killer (NK), and regulatory T (Treg) cells (J) and dendritic cells ($Ly6G^-MHCII^+F4/80^-CD11c^+$) (K) among $CD45^+$ leukocytes isolated from mock-treated mice and mice treated with 2 mg imiquimod daily for 6 days (n = 6–10 biological replicates/group).

(L) Proportion of colonic lamina propria $CX_3CR_1^{hi}$ macrophages among $CD45^+$ leukocytes in mock-treated mice and mice treated daily with 2 mg imiquimod for 3 (D3) and 6 days (D6) (n = 6–14 biological replicates/group). Data are presented as the mean ± SEM with $^*p < 0.05$, $^{**}p < 0.005$, and $^{***}p < 0.001$ by Mann-Whitney U test. See also Figures S1 and S2.

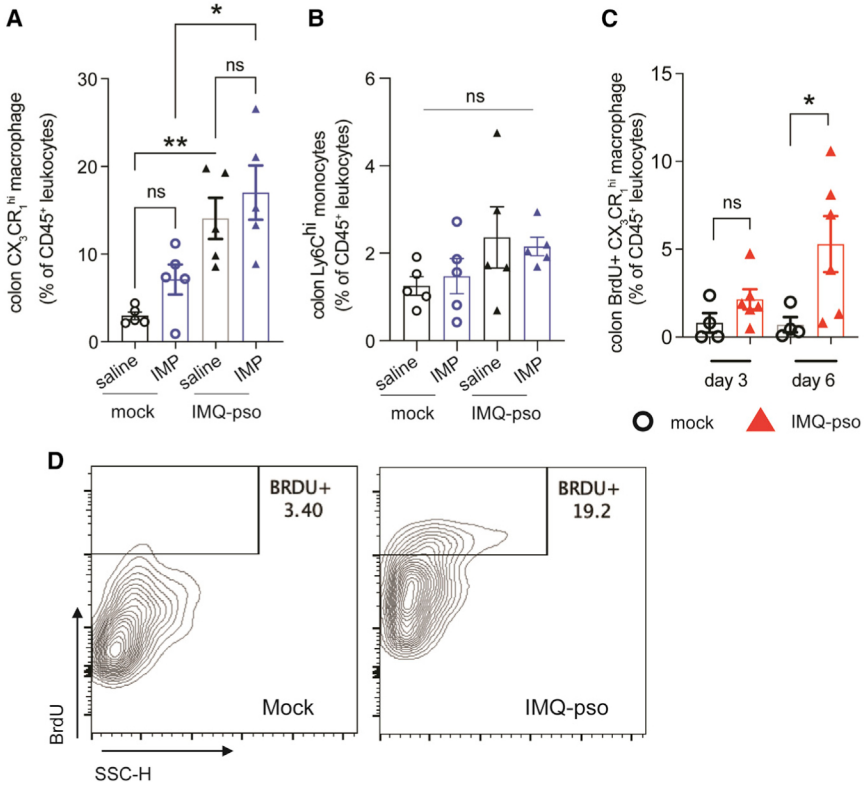

Figure 2. The increase in colonic $CX_3CR_1^{hi}$ macrophages in psoriasis is due to *in situ* macrophage proliferation and not to monocyte infiltration

(A and B) Proportions of $CX_3CR_1^{hi}$ macrophages (A) and $Ly6C^{hi}$ monocytes (B) among $CD45^+$ leukocytes in the colonic lamina propria of mice treated with 4.26×10^9 particles of polylactic-co-glycolic acid (PLGA)-negatively charged, carboxylated IMPs in 200 μL sterile PBS via daily tail vein injection and mock treatment on the back skin for 6 days (IMP mock); treated daily with 200 μL saline i.v. and mock treatment on the back skin for 6 days (saline mock); or treated daily with 4.26×10^9 IMPs in 200 μL sterile PBS i.v. and 2 mg imiquimod on the back skin for 6 days (IMP IMQ-pso) (n = 5 biological replicates/group).

(C and D) Proportions of colonic lamina propria $BrdU^+$ $CX_3CR_1^{hi}$ macrophages among $CD45^+$ leukocytes in mock-treated or IMQ-treated mice (IMQ) for 3 and 6 days (C). Representative flow cytometry plots from mock (left) and IMQ-pso mice (right) (D) (n = 4–6 biological replicates/group). Data are presented as the mean ± SEM; *p < 0.05, **p < 0.005 by Mann-Whitney U test.

mock-treated group (Figure 2A). This is consistent with the finding that IMQ-pso mice did not show increased monocyte infiltration in the colon (Figure 2B). Thus, the increased proportion of colonic $CX_3CR_1^{hi}$ macrophages in IMQ-pso is not due to the infiltration of blood-derived monocytes. To track the potential *in situ* proliferation of colonic macrophages during IMQ-pso, mice were injected intraperitoneally with 1 mg of bromodeoxyuridine (BrdU), a DNA-intercalating agent. Colonic lamina propria cells were isolated for flow cytometric analysis of $BrdU^+$ cells 4 h post-injection. This showed that the proportion of $BrdU^+$ colonic $CX_3CR_1^{hi}$ macrophages was significantly increased in mice with psoriasis, compared with control mice (Figure 2C; gating strategy in Figure 2D).

Taken together, these results show that the rise of colonic $CX_3CR_1^{hi}$ macrophages during psoriasis is linked to an increased *in situ* proliferation.

Increased $CX_3CR_1^{hi}$ macrophage proliferation in the colon during psoriasis is not due to oral uptake of imiquimod nor to circulating IL-17

It has previously been reported that unintended oral uptake of IMQ results in systemic effects observed in the IMQ-pso mouse model (Grine et al., 2016). To exclude a potential effect of oral ingestion of IMQ on colonic macrophages, truncated-cone-shaped Elizabethan collars (ECs) were placed around the necks of mice and IMQ was applied to the shaved dorsal skin as described above. Of note, IMQ-pso mice were always singly housed, excluding oral ingestion of IMQ by littermates. Importantly, these mice exhibited a similar increase in $CX_3CR_1^{hi}$ macrophages in the colon compared with their non-EC-wearing counterparts (Figure 3A). Further, there was no difference in disease severity (Figure 3B) or in the increased proportion of IL-17$^+$ γδ T cell populations in IMQ-pso mice with and without ECs (Figure 3C), indicating that oral uptake of IMQ was not driving psoriatic disease, as previously suggested (Grine et al., 2016). These findings demonstrate that the increase in colonic $CX_3CR_1^{hi}$ macrophages observed in psoriasis is linked to dermal inflammation following topical application of IMQ and not to potential gastrointestinal inflammation due to IMQ oral ingestion.

Increased levels of circulating IL-17A and IL-17F are commonly reported in patients with psoriasis (Brembilla et al., 2018; Fitz et al., 2018), as well as in IMQ-pso mice (Yang et al., 2013; Chen et al., 2017a; Takuathung et al., 2018; Xu et al., 2018). To determine if circulating IL-17A/F had an impact on colonic $CX_3CR_1^{hi}$ macrophage populations, mice were administered either 150 or 600 pg of IL-17A/F in 200 μL of saline intravenously daily. Since we observed an increase in $CX_3CR_1^{hi}$ macrophages by day 3 of disease, we administered IL-17A/F for 3 consecutive days. While IL-17A/F administration had no impact on colonic $CX_3CR_1^{hi}$ macrophages (Figures 3D and 3E), it led to an increased number of total splenocytes and to higher proportions and numbers of splenic neutrophils (Figure S3), which is consistent with previous reports of the role of IL-17 on neutrophil proliferation and recruitment (Schwarzenberger et al., 1998; Stoppelenburg et al., 2013). Under these experimental conditions, IL-17 does not contribute to the rise of colonic $CX_3CR_1^{hi}$ macrophages in psoriasis.

Thus, the rise of colonic $CX_3CR_1^{hi}$ macrophages in IMQ-pso is due neither to the oral ingestion of IMQ nor to the systemic increase of IL-17.

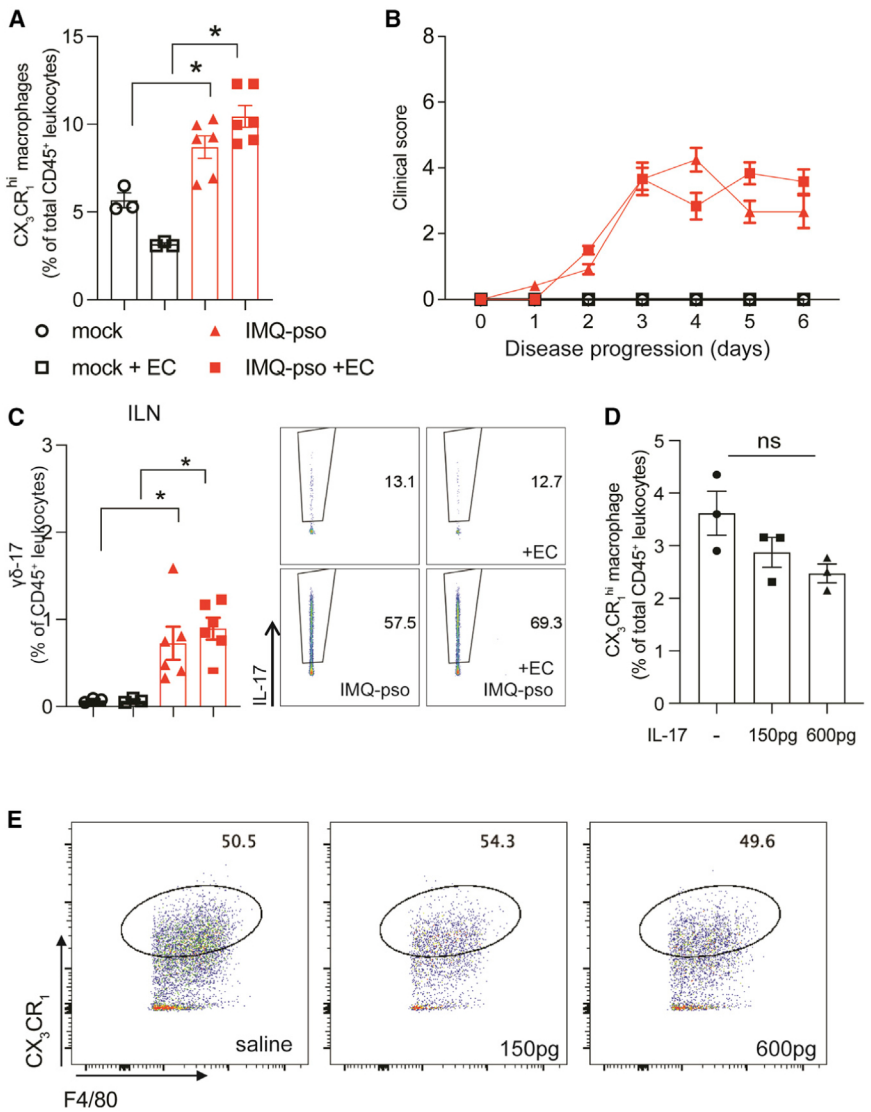

Figure 3. Increased $CX_3CR_1^{hi}$ macrophage proliferation in the colon during psoriasis is not due to oral uptake of imiquimod nor to circulating IL-17

(A) Proportions of $CX_3CR_1^{hi}$ macrophages among $CD45^+$ leukocytes in the colonic lamina propria of mock-treated mice or mice treated daily with 2 mg imiquimod (IMQ-pso) with and without Elizabethan collars (EC) (n = 3–6 biological replicates/group).

(B and C) Skin erythema and scaling were monitored in mice either treated daily with 2 mg imiquimod (IMQ-pso) or untreated (mock) with and without Elizabethan collars (EC) and given a clinical score (B). Proportions of γδ $IL\text{-}17^+$ T cells among total leukocytes ($CD45^+$ cells) were determined by flow cytometry after stimulation of cells isolated from the inguinal lymph node (ILN) (C) for 4 h with PMA (10 ng/mL), ionomycin (1 μg/mL), and brefeldin A (5 μg/mL) *ex vivo*, with representative plots shown (n = 3–6 biological replicates/group).

(D and E) IL-17A/F (150 and 600 pg in 200 μL saline) or saline (−) was administered i.v. in a total volume of 200 μL on 3 consecutive days and the proportions of colonic lamina propria $CX_3CR_1^{hi}$ macrophages among $CD45^+$ leukocytes were assessed by flow cytometry (D). Representative flow cytometry plots of $CX_3CR_1^{hi}$ macrophages from saline (left), 150 pg/mL (middle), and 600 pg/mL (right) IL-17A/F-treated mice (E) (n = 3 biological replicates/group). Results are shown as the mean ± SEM. *$p < 0.05$ by Kruskal-Wallis test. See also Figure S3.

The enrichment of colonic $CX_3CR_1^{hi}$ macrophages in IMQ-pso is linked to changes in the gut microbiota

The gut microbiota has a dramatic impact on the host immune system, both locally and systemically (Lazar et al., 2018; Tan et al., 2021). To determine whether the gut microbiota affected colonic $CX_3CR_1^{hi}$ macrophages, we compared their proportions in germ-free (GF) versus specific-pathogen-free (SPF) mice. Absence of gut microbiota in GF mice was associated with a statistically significant reduction in the proportion of $CX_3CR_1^{hi}$ macrophages to approximately 30% of that seen in SPF mice (Figure 4A), suggesting that this immune subset is regulated by the gut microbiota. To determine whether the changes in the gut microbiota during psoriasis contributed to the increase in colonic $CX_3CR_1^{hi}$ macrophages, we reconstituted GF mice with cecal contents from mock-treated mice or IMQ-pso mice and analyzed the recipient mice 5 weeks after transfer. GF mice recolonized with mock or IMQ-pso-derived microbiota had drastically different gut microbiota compositions (Figure S4A), but respectively deviated from that of their donors (Figure S4B). This was predominantly due to a shift in the relative abundance of taxa and not to the introduction or disappearance of taxa, as the majority of taxa were preserved between the recipient and the donor mice (Figure S4C). Cecal transfers from IMQ-pso donor mice increased the proportions of $CX_3CR_1^{hi}$ macrophages in the colon of GF mice, compared with those receiving cecal transfers from mock-treated mice (Figure 4B). This result suggests that microbiota composition regulates $CX_3CR_1^{hi}$ macrophages in the colon. The shift in the gut microbiota composition between the donor and the recipient mice may explain the subtle effect observed on the colonic $CX_3CR_1^{hi}$ macrophages. To confirm the role of the gut microbiota on the proliferation of $CX_3CR_1^{hi}$ macrophages during IMQ-pso, we treated SPF mice with broad-spectrum antibiotics 1 week before and during the induction of IMQ-pso. While all mice developed psoriasis (data not shown), colonic $CX_3CR_1^{hi}$ macrophages were significantly increased in SPF mice only, but not in SPF mice treated with antibiotics (Figure 4C), demonstrating the role of the gut microbiota on this cell subset. Together, these results demonstrate the role of dysbiosis in IMQ-pso on the proliferation of colonic $CX_3CR_1^{hi}$ macrophages.

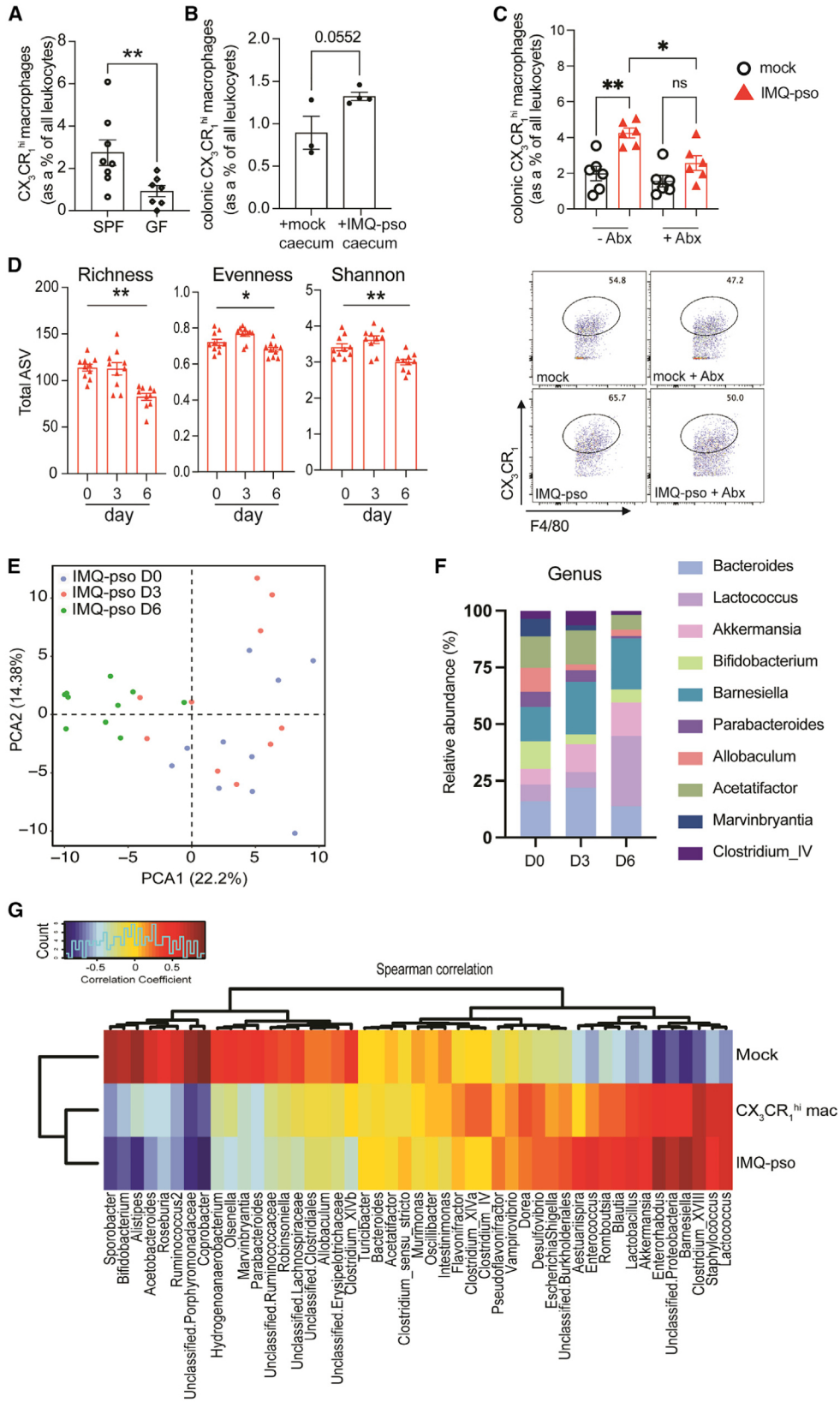
A
CX3CR1hi macrophages (as a % of all leukocytes)
**
SPF
GF
B
colonic CX3CR1hi macrophages (as a % of all leukocytes)
0.0552
+mock caecum
+IMQ-pso caecum
C
colonic CX3CR1hi macrophages (as a % of all leukocytes)
**
ns
*
mock
IMQ-pso
- Abx
+ Abx
D
Richness
Evenness
Shannon
Total ASV
day
54.8
47.2
mock
mock + Abx
65.7
50.0
IMQ-pso
IMQ-pso + Abx
CX3CR1
F4/80
E
IMQ-pso D0
IMQ-pso D3
IMQ-pso D6
PCA2 (14.38%)
PCA1 (22.2%)
F
Genus
Relative abundance (%)
D0
D3
D6
Bacteroides
Lactococcus
Akkermansia
Bifidobacterium
Barnesiella
Parabacteroides
Allobaculum
Acetatifactor
Marvinbryantia
Clostridium_IV
G
Count
Correlation Coefficient
Spearman correlation
Mock
CX3CR1hi mac
IMQ-pso
Sporobacter
Bifidobacterium
Alistipes
Acetobacteroides
Roseburia
Ruminococcus2
Unclassified.Porphyromonadaceae
Coprobacter
Hydrogenoanaerobacterium
Olsenella
Marvinbryantia
Parabacteroides
Unclassified.Ruminococcaceae
Robinsoniella
Unclassified.Lachnospiraceae
Unclassified.Clostridiales
Allobaculum
Unclassified.Erysipelotrichaceae
Clostridium_XlVb
Turicibacter
Bacteroides
Acetatifactor
Clostridium_sensu_stricto
Murimonas
Oscillibacter
Intestinimonas
Flavonifractor
Clostridium_XlVa
Clostridium_IV
Pseudoflavonifractor
Vampirovibrio
Dorea
Desulfovibrio
EscherichiaShigella
Unclassified.Burkholderiales
Aestuariispira
Enterococcus
Romboutsia
Blautia
Lactobacillus
Akkermansia
Enterorhabdus
Unclassified.Proteobacteria
Barnesiella
Clostridium_XVIII
Staphylococcus
Lactococcus

Psoriasis has previously been linked to changes in gut microbiota composition, particularly a loss of bacterial diversity in patients (Scher et al., 2015; Codoner et al., 2018). Using 16S rRNA sequencing, we similarly identified a significant decrease in gut bacterial richness by day 6 in psoriasis (Figure 4D). Further, microbiota composition was significantly shifted in mice treated with IMQ by day 3 (Table S2), the time point at which enrichment of $CX_3CR_1^{hi}$ macrophages was also observed (Figure 1L), with an even greater shift at day 6 (Figure 4E). At the genus level (Figure 4F), *Akkermansia, Clostridium XVIII*, and *Lactococcus* were among those significantly increased at day 6, while *Allobaculum* was significantly decreased (Figure 4F and Table 1). Spearman's correlation analysis also revealed that these bacteria were highly correlated with both psoriasis severity and proportion of colonic CX_3CR1^{hi} macrophages (Figure 4G). These results indicate that psoriasis is associated with a dysbiotic microbiota composition, which impairs colonic $CX_3CR_1^{hi}$ macrophage homeostasis.

Psoriasis leads to increased bacterially derived succinate, which promotes the proliferation of colonic $CX_3CR_1^{hi}$ macrophages

The gut microbiota has been shown to shape host immunity through the release of metabolites such as SCFA. To determine the mechanism by which a psoriasis-associated microbiota regulates $CX_3CR_1^{hi}$ macrophages, we quantified microbiota-derived metabolites in the cecal content of IMQ-pso versus control mice by nuclear magnetic resonance (NMR) and found no differences in levels of bacterial metabolites, acetate, butyrate, and propionate or in lactate (Figures 5A–5D). However, we found that both pyruvate and succinate levels were increased in IMQ-pso mice, with only succinate reaching statistical significance (Figures 5E and 5F). Using PiCRUST analysis to predict the metagenomic function of the gut microbiota, we observed enrichment of succinate-producing pathways in the IMQ-pso microbiota. The major pathway for the anaerobic production of succinate is via the metabolism of phosphoenolpyruvic acid (PEP) or pyruvate, which yields oxaloacetate that is further metabolized into malate, fumarate, and succinate (Figure 5G) (Fernandez-Veledo and Vendrell, 2019). By examining KEGG ortholog groups (KOs) associated with this pathway (Table S3), we found that 10 of 13 KOs associated with succinate production were enriched in the microbiota of mice at day 3 of psoriasis, compared with untreated mice, with none considered statistically significant (Figure 5H). However, at day 6 of psoriasis, all 13 KOs associated with succinate production were enriched, compared with untreated groups, with 9 considered statistically significant (Figure 5I). To investigate which taxa potentially contribute to succinate production in IMQ-pso animals, we first identified which amplicon sequence variants (ASVs) contributed to the 13 KOs associated with succinate-producing pathways (Figure 5G). Among the 227 relevant ASVs, *Lactococcus*, *Acetatifactor*, *Clostridium XVIII*, *Lactobacillus*, and *Aestuariispira* were significantly enriched in IMQ-pso mice compared with mock animals (Table 2).

Thus, psoriasis is associated with a gut microbiota that has a greater capacity for succinate production.

To confirm this, we recolonized GF mice with microbiota from control or IMQ-pso mice and found that animals recolonized with the latter had higher cecal succinate levels than GF mice recolonized with control microbiota at 3 weeks post-colonization (Figure 5J). Like IMQ-pso mice (Figures 5A–5F), GF mice recolonized with IMQ-pso microbiota also had increased levels of pyruvate, while no changes were observed for other metabolites, such as the SCFAs acetate, butyrate, and propionate, as well as lactate (Figure S4D). This confirms the higher potential of microbiota associated with psoriasis to produce succinate. As GF mice had a lower proportion of colonic $CX_3CR_1^{hi}$ macrophages (Figure 4A), in parallel with lower succinate levels (Figure 5K), we hypothesized that succinate may regulate the colonic $CX_3CR_1^{hi}$ macrophage population by regulating either their *in situ* proliferation or their survival. Colonic lamina propria cells were cultured at 1×10^6 cells per well for 72 h and incubated with 500 μM succinate, with PBS as a negative control. Since Ki67 is expressed in a graded manner in proliferation (Miller et al., 2018), the median fluorescence intensity (MFI) of Ki67 was used to indicate proliferation. Succinate significantly increased the Ki67 MFI in $CX_3CR_1^{hi}$ macrophages, showing that succinate can promote colonic $CX_3CR_1^{hi}$ macrophage proliferation (Figure 5L). These findings were confirmed under hypoxic conditions (3% O_2), which better reflect the intestinal lamina propria environment (Zeitouni et al., 2016) (Figure 5M). Of note, succinate did not affect the expression of the survival marker Bcl-2 in $CX_3CR_1^{hi}$ macrophages (Figure 5N), suggesting that succinate affects their proliferation rather than their survival.

Taken together, this work shows a role for succinate in promoting the proliferation of homeostatic $CX_3CR_1^{hi}$ macrophages.

Figure 4. The enrichment of colonic $CX_3CR_1^{hi}$ macrophages in IMQ-pso is linked to changes in gut microbiota

(A) Proportions of colonic lamina propria $CX_3CR_1^{hi}$ macrophages among $CD45^+$ leukocytes in specific-pathogen-free (SPF) and germ-free (GF) mice (n = 7–8 biological replicates/group).

(B) Proportions of colonic lamina propria $CX_3CR_1^{hi}$ macrophages among $CD45^+$ leukocytes in GF mice recolonized for 5 weeks with fresh cecal content immediately after isolation, from either mock-treated mice (GF +mock) or mice treated daily with 2 mg imiquimod for 6 days (GF +IMQ-pso) (n = 3–4 biological replicates/group).

(C) Proportions of colonic lamina propria $CX_3CR_1^{hi}$ macrophages among $CD45^+$ leukocytes in SPF mock-treated mice or mice treated daily with 2 mg imiquimod (IMQ-pso) with and without antibiotic treatment (Abx) for 2 weeks before IMQ-pso and during disease (n = 6 biological replicates/group).

(D–F) Impact of IMQ-pso on the gut microbiota was determined by 16S rRNA gene sequencing of fecal samples from mice treated daily for 0, 3, or 6 days following treatment with 2 mg imiquimod. Alpha diversity of gut microbiota as assessed by richness, evenness, and Shannon diversity index (D). Beta diversity was assessed by principal coordinate analysis (PCA) of Aitchison distances between individual singly housed mice at day 6 (E). Relative average abundance at the genus level at days 0, 3, and 6 of IMQ-pso. The top 10 represented genera are listed (F) (n = 10 biological replicates/group).

(G) Spearman's correlation between microbial genus enrichment and mock-treated mice (top, n = 5), colonic lamina propria $CX_3CR_1^{hi}$ macrophage proportion determined by flow cytometry (middle), and IMQ-pso clinical score at day 6 (bottom, n = 10) (n = 6 biological replicates/group). Results are shown as the mean ± SEM. *$p < 0.05$, **$p < 0.005$ by Mann-Whitney U test. See also Figure S4 and Table S2.

Table 1. Aldex2 differential abundance test between day 0 and day 6 IMQ-pso-treated mice at the genus level, related to Figure 4

Genus	Median CLR (center log-ratio), IMQ-pso D0	Median CLR, IMQ-pso D6	Effect size	FDR (Welch's t test)	FDR (Wilcoxon test)
Bacteroides	4.889977	8.104169	−1.22477	0.004835	0.006545
Lactococcus	3.672151	9.537485	−1.73427	0.00055	0.001194
Akkermansia	3.236105	7.860071	−1.13413	0.003961	0.004468
Bifidobacterium	4.395444	3.943091	0.079182	0.526397	0.870146
Barnesiella	4.749567	8.982965	−1.54726	0.001137	0.002221
Parabacteroides	3.74432	1.588452	0.367993	0.242166	0.341258
Allobaculum	3.670826	4.073294	−0.10167	0.893074	0.773734
Olsenella	2.978653	3.458837	−0.18815	0.759678	0.628756
Acetatifactor	4.844319	7.4512	−1.26469	0.005382	0.003774
Marvinbryantia	3.790853	−0.08455	0.745537	0.039048	0.040144
Desulfovibrio	2.723892	5.450233	−1.23059	0.004961	0.005232
Lactobacillus	1.362048	6.271582	−1.89395	0.000723	0.001397
Clostridium sensu stricto	−6.66115	5.972197	−1.02172	0.015602	0.011313
Clostridium XVIII	−1.39315	5.706078	−1.81415	0.000922	0.000268
Clostridium IV	3.00479	5.172939	−0.57864	0.267329	0.044986
Romboutsia	−6.48625	6.820819	−0.92422	0.027323	0.019418
Clostridium XIVa	2.336934	5.617456	−1.58142	0.001114	0.00102
Coprobacter	3.135549	−4.56112	1.948449	0.000968	0.000261
Vampirovibrio	−6.33971	3.354496	−0.76545	0.060195	0.039097
Acetobacteroides	1.261223	−0.4358	0.319372	0.296157	0.541854
Robinsoniella	−1.55154	−2.73937	0.010393	0.791562	0.858914
Dorea	0.903527	5.503122	−1.54102	0.00104	0.001585
Ruminococcus2	0.685543	−0.1541	0.095634	0.777767	0.77897
Alistipes	1.072051	0.317296	0.364162	0.151533	0.291329
Aestuariispira	−7.34882	2.876462	−1.41939	0.001825	0.001894
Turicibacter	−7.12635	−2.16593	−0.61171	0.13993	0.139551
Oscillibacter	1.019239	2.319928	−0.31575	0.572556	0.407066
Sporobacter	−0.28808	−4.83931	0.866133	0.066486	0.033907
Pseudoflavonifractor	−0.19865	0.623517	−0.20417	0.767497	0.734361
Blautia	−4.37885	1.612353	−0.72235	0.097457	0.078698
Intestinimonas	−1.29478	0.8772	−0.33671	0.498144	0.346826
Murimonas	−1.5708	0.015055	−0.34053	0.38193	0.281544
Clostridium XIVb	−0.94605	−1.00541	0.032086	0.605244	0.766668
Flavonifractor	−5.76396	−3.56948	−0.17093	0.61163	0.685284
Enterococcus	−8.20104	−0.82965	−1.34009	0.00914	0.010094
Staphylococcus	−6.41676	0.779789	−0.72848	0.078241	0.079064
Pseudomonas	−2.46372	−4.8179	0.778571	0.051986	0.080246
Enterorhabdus	−2.75941	2.413445	−1.44708	0.004071	0.001035
Roseburia	−7.19114	−4.638	−0.31946	0.453908	0.465455
Hydrogenoanaerobacterium	−1.96721	−4.28241	0.499338	0.232593	0.189406
Anaerotruncus	−7.96709	−4.88142	−0.48731	0.290968	0.262989
Escherichia/Shigella	−8.16028	−3.9943	−0.83248	0.073534	0.074276
Anaerostipes	−5.46524	−4.93146	0.054992	0.683077	0.746897

IMQ-induced psoriasis predisposes mice to exacerbated DSS colitis

$CX_3CR_1^{hi}$ macrophages are immunomodulatory through their production of cytokines such as IL-10, TNF, and TGF-β (Bain et al., 2012; Zigmond et al., 2014). Thus, we investigated whether changes in $CX_3CR_1^{hi}$ macrophage homeostasis in psoriasis affected the colonic cytokine environment. By qPCR of whole colon tissue, we identified significantly increased expression of

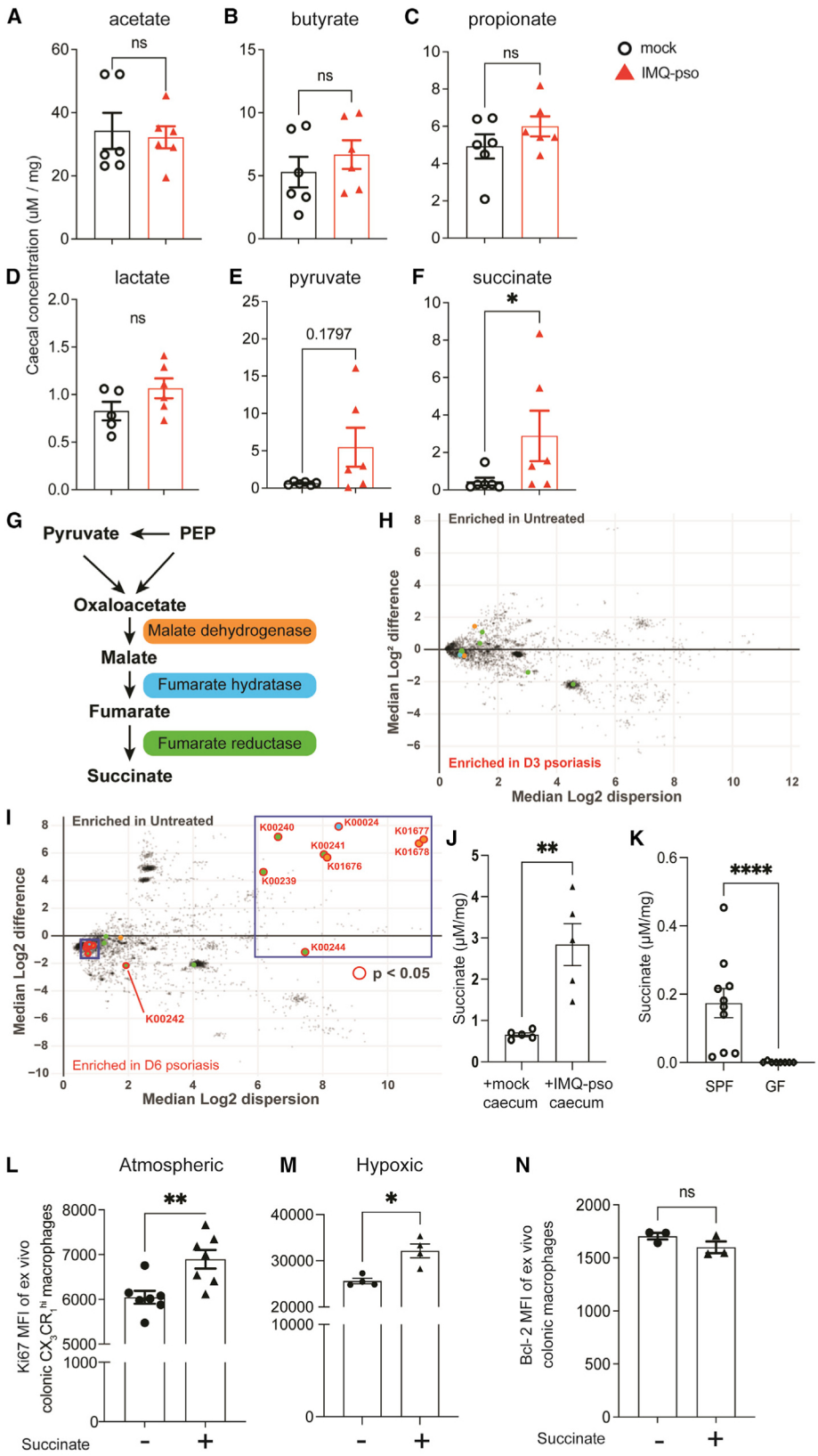
A
acetate
ns
B
butyrate
ns
C
propionate
ns
mock
IMQ-pso
Caecal concentration (uM / mg)
D
lactate
ns
E
pyruvate
0.1797
F
succinate
*
G
Pyruvate
PEP
Oxaloacetate
Malate dehydrogenase
Malate
Fumarate hydratase
Fumarate
Fumarate reductase
Succinate
H
Enriched in Untreated
Enriched in D3 psoriasis
Median Log² difference
Median Log2 dispersion
I
Enriched in Untreated
K00240
K00024
K01677
K00241
K01678
K01676
K00239
K00244
K00242
p < 0.05
Enriched in D6 psoriasis
Median Log2 difference
Median Log2 dispersion
J
**
Succinate (µM/mg)
+mock caecum
+IMQ-pso caecum
K
****
Succinate (µM/mg)
SPF
GF
L
Atmospheric
**
Ki67 MFI of ex vivo colonic CX3CR1int macrophages
Succinate
M
Hypoxic
*
N
ns
Bcl-2 MFI of ex vivo colonic macrophages
Succinate

TNF (*Tnf*), IL-10 (*Il10*), and TGF-β (*Tgfb*) (Figures 6A–6C), while IFN-γ (*Ifng*) and IL-22 (*Il22*) remained unchanged (Figures 6D and 6E), suggesting that a protective or repair process may be taking place. These changes in the cytokine milieu were not linked to psoriasis-induced systemic inflammation, as intravenous administration of IL-17 had no impact on the expression of these genes or on bacterial metabolites (Figures S5A–S5F), and so they were likely due to production by the enriched $CX_3CR_1^{hi}$ macrophage population. To determine whether psoriasis is similarly associated with changes in $CX_3CR_1^{hi}$ macrophage-derived cytokines in humans, we extracted data for gene set enrichment analysis of sigmoidal gut biopsy sample transcriptomes (GEO: GSE150851) and found enriched signals in the gene set related to TNF signaling in patients with psoriasis (Figure 6F), as observed in the IMQ-pso mouse model.

Patients with psoriasis have a higher risk of developing IBD, and IBD is characterized by higher TLR activation due to changes in the gut microbiota composition (Erridge et al., 2010; Cottone et al., 2019). To determine whether the gut microbiota from IMQ-pso mice can differentially activate TLR, we used HEK-Blue TLR4 and HEK-Blue TLR2 reporter cell lines in which the intensity of TLR4 and TLR2 activation is quantified through a colorimetric assay. HEK cells were incubated with suspended feces from control versus IMQ-pso mice, and we found that microbiota from IMQ-pso activated both TLR2 and TLR4 to a greater extent (Figures 6G, 6H, S5G, and S5H), suggesting that these mice have gut microbiota with higher inflammatory potential. GF mice had significantly lower activation of TLR using the HEK-Blue reporter cell lines (Figure S5I), highlighting the suitability of the assay for measuring intestinal TLR content. Similarly, genes of the NF-κB pathway, downstream of TLR activation, are enriched in the colon of patients with psoriasis, suggesting a potential "pro-inflammatory gut microbiota" in these patients as well (Figure 6I). Despite a more inflammatory gut microbiota, IMQ-pso mice did not develop evidence of spontaneous colitis, in that colon length was not reduced (Figure 6J), and they had a similar infiltration of $Ly6C^{hi}$ monocytes (Figure 6K). The fact that IMQ-pso mice had similar profiles of expression of tight junction protein (*Tjp1*), occludin (*Ocln*), and the mucus marker *Muc2* (Figure S6A) suggests a "preserved" separation of host-gut microbiota, with limited TLR activation by gut bacterial ligands. This could explain why these mice do not develop spontaneous colitis. The limited interaction between the gut microbiota and the host was confirmed, with similar expression of anti-microbial peptides RegIIIγ (*Reg3g*), cathelin-related antimicrobial peptide (*Camp*), β-defensin-3 (*Defb3*), and β-defensin-14 (*Defb14)* (data not shown), although MMP7 (*Mmp7*) (Figure 6L) was upregulated in IMQ-pso mice. MMP7 is an enzyme involved in epithelial repair (Hayden et al., 2011) and has been reported to be upregulated in IBD (Derkacz et al., 2021), suggesting that in psoriasis, compensatory mechanisms, such as increases in MMP7 and $CX_3CR_1^{hi}$ macrophages (Schneider et al., 2015), may be in place to maintain gut homeostasis.

Elevated succinate and MMP7, both increased in IMQ-Pso mice, have been associated with IBD (Connors et al., 2018; Derkacz et al., 2021). While $CX_3CR_1^{hi}$ macrophages are homeostatic and hyporesponsive to TLR stimulation (Schneider et al., 2015), under challenge conditions they can become pro-inflammatory by recruiting inflammatory monocytes in both chemically and bacterially induced colitis (He et al., 2019). We thus hypothesized that the colonic environment in psoriasis may be primed for IBD under additional challenge conditions. To test this hypothesis, we used DSS as the challenge, as this chemical impairs epithelial integrity, increasing bacterial translocation and thus inflammation, as observed in human IBD. Mice were treated with IMQ-pso for 6 days, and from day 3 onward, when $CX_3CR_1^{hi}$ macrophages are found in higher proportion, we supplemented the drinking water with 3% DSS for 5 days (Figure 6M). IMQ-pso mice developed significantly more severe colitis, particularly at later stages of the DSS treatment, as shown by their clinical score (Figure 6N). Disease progression at day 5 was so severe in the IMQ-pso group that the experiment was ended at day 5, rather than day 7, due to ethical concerns, while significant differences in weight were not observed (Figure 6O). Accordingly, colon length was significantly shorter in IMQ-pso mice (Figure 6P) and colonic immune cell infiltration more pronounced in these mice (Figures 6Q and 6R). We found that the gut microbiota of both mock and IMQ-pso mice were significantly shifted after DSS treatment and were similar between groups (IMQ-pso + DSS versus mock + DSS) (Figures S6B–S6C), with no differentially abundant taxa identified at the genus level (data not shown). This indicates that worsened DSS colitis in

Figure 5. Psoriasis leads to increased bacterially derived succinate, which promotes the proliferation of colonic $CX_3CR_1^{hi}$ macrophages

(A–F) Concentration of cecal metabolites, acetate (A), butyrate (B), propionate (C), lactate (D), pyruvate (E), and succinate (F), assessed by NMR in cecal contents from mock-treated mice and mice treated daily with 2 mg imiquimod (IMQ-pso) for 6 days, normalized per milligram of cecal content (n = 6 biological replicates/group).

(G–I) Depiction of the major pathway for the anaerobic production of succinate. Pyruvate or phosphoenolpyruvic acid (PEP) can be metabolized into oxaloacetate, which is further metabolized into malate (by malate dehydrogenase; orange), fumarate (fumarate hydratase; blue), and succinate (fumarate reductase; green) (G). Differential abundance testing by Aldex2 of PICRUSt2-predicted KEGG ortholog (KO) between mock-treated mice and mice treated daily with 2 mg imiquimod for 3 (H) or 6 days (I). KOs associated with succinate production are highlighted (n = 6–10 biological replicates/group).

(J) Succinate concentration was measured by NMR in cecum isolated from GF mice 3 weeks after their recolonization by oral administration with cecal contents from mock-treated mice (GF +mock) or mice treated daily for 6 days with 2 mg of imiquimod (GF +IMQ-pso), normalized per milligram of cecal content (n = 5 biological replicates/group).

(K) Succinate concentration measured by NMR in cecal samples of GF and SPF mice normalized per milligram of cecal content (n = 10 biological replicates/group).

(L–N) Colonic $CX_3CR_1^{hi}$ macrophages were stimulated *ex vivo* for 72 h ±0.5 M succinate and Ki67 MFI was measured by flow cytometry in cells cultured under atmospheric (L) and 3% O_2 (hypoxic) (M) conditions. Bcl-2 MFI was assessed in $CX_3CR_1^{hi}$ colonic macrophages cultured under atmospheric conditions (N) (n = 3–10 biological replicates/group). Results are shown as the mean ± SEM; *p < 0.05, **p < 0.005, ****p < 0.0001 by Mann-Whitney U test. See also Figure S5 and Table S3.

Table 2. Differentially enriched taxa involved in the succinate-producing pathway at the amplicon sequence variant level as tested by Aldex2 differential abundance analysis, related to Figure 5

ASV	Taxa	Median CLR (center log-ratio), IMQ-pso D0	Median CLR, IMQ-pso D6	Effect size	FDR (Welch's t test)	FDR (Wilcoxon test)
TACGTAGGTCCCGAGCGTTGTCCG GATTTATTGGGCGTAAAGCGAGCG CAGGTGGTTTATTAAGTCTGGTGTA AAAGGCA	*Lactococcus garvieae/lactis/ taiwanesis*	9.083423039	12.13080662	−1.20198	0.019027	0.026069
TACGTAGGGGGCGAGCGTTATCCG GATTCACTGGGTGTAAAGGGAGCG TAGACGGCCATGCAAGCCAGGGGT GAAAGCCC	*Acetatifactor*	6.960105	8.182026791	−1.09426	0.026712	0.030853
TACGTAGGTGGCAAGCGTTATCCGG AATTATTGGGCGTAAAGAGGGAGCA GGCGGCAGCAAAGGTCTGTGGTGAA AGACT	*Clostridium XVII cocleatum*	3.657664175	8.433130886	−1.23541	0.025115	0.007138
TACGTAGGTGGCAAGCGTTATCCGGA TTTATTGGGCGTAAAGGGAACGCAGG CGGTCTTTTAAGTCTGATGTGAAAGCCT	*Lactobacillus animalis/ apodemi/crispatus/ faecis/murinus*	3.678286294	7.691048346	−1.33566	0.014389	0.030162
TACGAAGGGGGCAAGCGTTGTTCGGA ATTACTGGGCGTAAAGGGAGTGTAGGC GGTTTAGTAAGATAGTGGTGAAATCCC	*Aestuariispira*	−2.222851381	5.583387277	−1.22092	0.02536	0.029137

IMQ-pso mice was not driven by changes in the gut microbiota composition upon DSS treatment.

Together, these results highlight the disrupted gut immune environment in psoriasis, which primed for aggravated colitis development under DSS challenge.

DISCUSSION

The interaction between the host and its gut microbiota is complex and finely balanced, with disruption of one affecting the other. In the current work, we show that psoriasis in the IMQ-pso mouse model disturbs both the gut microbiota composition and its activity. The IMQ-pso-associated microbiome exhibited higher inflammatory potential and produced higher levels of the metabolite succinate. In parallel, there was an increased *in situ* proliferation of colonic $CX_3CR_1^{hi}$ macrophages *in vivo*, likely as a result of elevated succinate, which induces their proliferation *in vitro*. $CX_3CR_1^{hi}$ macrophages play a key role in maintaining gut homeostasis but can also aggravate colitis development under infectious or chemically induced colitis (He et al., 2019). When challenged with DSS, a compound that compromises the gut epithelium, IMQ-pso mice developed more severe colitis. This suggests a two-hit requirement in which psoriasis induces changes in the gut environment that prime for the development of IBD if additional environmental challenges are encountered. These findings provide insights into the reasons behind the high incidence of IBD in psoriasis patients. Our work shows that psoriasis exerts a causative effect and suggests that restoring a healthy gut microbiota in these patients may be a strategy to prevent IBD development.

Dysbiosis is a feature of most non-communicable diseases. However, it is unclear how dysbiosis develops and whether dysbiosis is a cause or consequence of disease. Here, we show that psoriasis causes dysbiosis, and this dysbiosis predisposes mice to aggravated colitis following DSS challenge. Altered gut microbiota has previously been reported in IMQ-pso mice, although whether these changes were protective or worsened disease was not explored (Shinno-Hashimoto et al., 2021). Another study reported that both GF and antibiotic-treated mice developed less severe psoriasis in a model of IMQ-pso compared with SPF mice due to a reduced Th17 response (Zakostelska et al., 2016). This suggests a detrimental role of the gut microbiota in the IMQ-pso model. We observed that the microbiota of IMQ-pso animals was more inflammatory, with a higher ability to activate TLR2 and TLR4, which likely contributed to the more severe DSS-induced colitis. The fact that the NF-κB activation pathway is enriched in the colon of patients with psoriasis suggests that, as in mice, psoriasis-associated gut microbiota of patients may also be enriched in TLR ligands. This warrants further investigation.

We also identified that the activity of the gut microbiota was shifted, with higher production of succinate in mice with psoriasis associated with the enrichment in succinate producing bacteria, such as *Lactobacillus animalis* (Shinno-Hashimoto et al., 2021). The increased colon length in IMQ-pso mice confirmed the increased fermentative activity of the microbiota commonly associated with succinate production (Armstrong et al., 2021). Increased microbiota-derived succinate has been reported in other non-communicable diseases such as IBD and associated comorbidities, including arthritis and calcium oxalate kidney stones (Fremder et al., 2021), as well as in obesity, a condition in which increased numbers of pro-inflammatory intestinal macrophages were reported (Rohm et al., 2021, 2022). While succinate can be used as a source of nutrients for intestinal pathogen

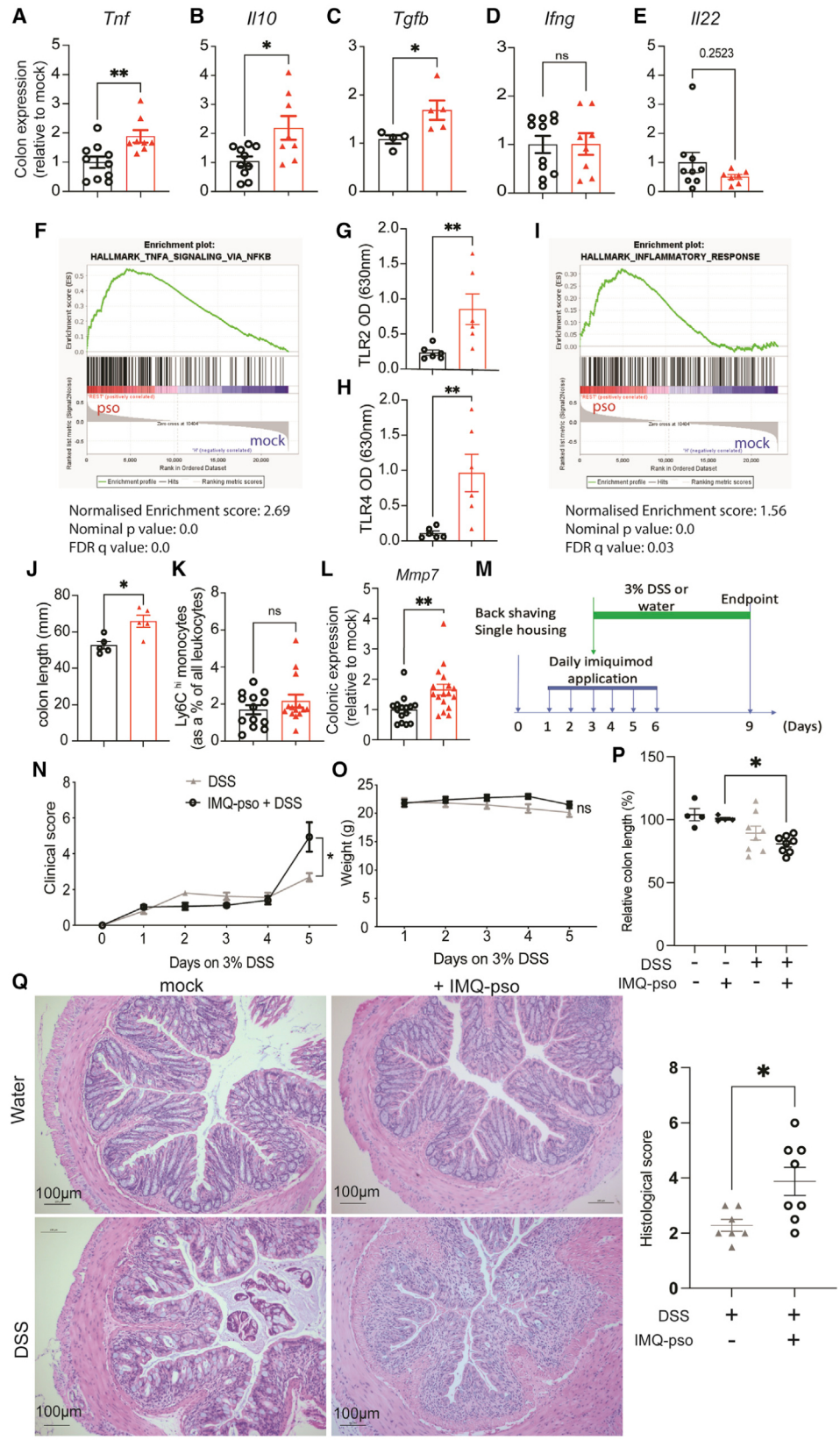
A
Tnf
B
Il10
C
Tgfb
D
Ifng
E
Il22
Colon expression (relative to mock)
**
*
*
ns
0.2523
F
Enrichment plot:
HALLMARK_TNFA_SIGNALING_VIA_NFKB
pso
mock
Normalised Enrichment score: 2.69
Nominal p value: 0.0
FDR q value: 0.0
G
TLR2 OD (630nm)
H
TLR4 OD (630nm)
I
Enrichment plot:
HALLMARK_INFLAMMATORY_RESPONSE
pso
mock
Normalised Enrichment score: 1.56
Nominal p value: 0.0
FDR q value: 0.03
J
colon length (mm)
K
Ly6C hi monocytes (as a % of all leukocytes)
ns
L
Mmp7
Colonic expression (relative to mock)
M
Back shaving
Single housing
3% DSS or water
Endpoint
Daily imiquimod application
(Days)
N
DSS
IMQ-pso + DSS
Clinical score
Days on 3% DSS
O
Weight (g)
ns
Days on 3% DSS
P
Relative colon length (%)
DSS
IMQ-pso
Q
mock
+ IMQ-pso
Water
DSS
100µm
Histological score
DSS
IMQ-pso

colonization or proliferation (Fernandez-Veledo and Vendrell, 2019; Fremder et al., 2021), it may also contribute to the stable colonization by pathobionts, perpetuating dysbiosis in psoriasis. Targeting succinate-producing bacteria may thus be a strategy to restore a healthy gut microbiota in psoriasis.

What triggered dysbiosis in our IMQ-pso cohort is unclear. While host inflammatory status can contribute to gut microbiota disturbances, IL-17 alone did not mimic the effects of psoriasis on bacterial succinate production. Thus, other host factors yet to be identified must be responsible. We have previously shown that high succinate levels under high protein feeding conditions led to increased B cell recruitment in the small intestine (Tan et al., 2022).

In the present work, we identified that dysbiosis and high colonic succinate contributed to the increased numbers of colonic $CX_3CR_1^{hi}$ macrophages *in vivo*. Both the recolonization of GF mice with IMQ-Pso microbiota and the antibiotic treatment of SPF mice during psoriasis induction established the role of the gut microbiota in the increase in colonic $CX_3CR_1^{hi}$ macrophages. This was independent of monocyte recruitment, but due to the *in situ* proliferation of colonic $CX_3CR_1^{hi}$ macrophages, with our *in vitro* data suggesting that succinate may directly contribute to $CX_3CR_1^{hi}$ macrophage proliferation. Succinate has previously been shown to shift macrophage and mesenchymal stem cell metabolic activity from oxidative phosphorylation to glycolysis, promoting respectively a pro-inflammatory state (Tannahill et al., 2013) and cell proliferation (Mao et al., 2020). Succinate may thus induce $CX_3CR_1^{hi}$ macrophage proliferation through similar metabolic effects. Another mechanism of action could be through the specific activation of the G-protein-coupled receptor 91 by succinate, which has been shown to promote macrophage IL-1β production (Littlewood-Evans et al., 2016) and endothelial cell proliferation (de Castro Fonseca et al., 2016). The observation that only $CX_3CR_1^{hi}$ macrophages proliferated in response to succinate may be due to succinate being delivered directly to macrophages, as previously shown (Fremder et al., 2021). However, while succinate has been shown to activate macrophages (Fremder et al., 2021), mice with psoriasis do not develop spontaneous colitis and have levels of colonic IL-22 similar to those of controls, suggesting preservation of gut homeostasis. We found that the enzyme MMP7 was upregulated in psoriasis in mice and is also enriched in the colons of patients with IBD (Derkacz et al., 2021). The fact that metalloproteinases, particularly MMP7, are involved in epithelial repair (Hayden et al., 2011) suggests that dysbiosis in psoriasis may affect the epithelial integrity, which is actively maintained by $CX_3CR_1^{hi}$ macrophages. Thus, the proliferation of $CX_3CR_1^{hi}$ macrophages may be a compensatory mechanism to preserve gut homeostasis in this dysbiotic environment. Similarly, while TNF is important for intestinal homeostasis, overproduction is a hallmark of colitis (Muzes et al., 2012), and anti-TNF therapy is an effective treatment for patients (Hanauer et al., 2002). This compensation may predispose to exacerbated inflammation when an additional challenge targeting the epithelium, such as DSS, is encountered. Indeed, $CX_3CR_1^{hi}$ macrophages have been shown to be highly immunogenic in models of 2,4,6-Trinitrobenzenesulfonic acid (TNBS), DSS (He et al., 2019), or *Salmonella*-induced colitis (Koscsó et al., 2020), and could also play an active role in monocyte recruitment through the release of CCL2 (He et al., 2019). Mice lacking CX_3CR_1 are protected from DSS colitis development, according to one report (Kostadinova et al., 2010), and subject to worse disease outcomes according to another (Medina-Contreras et al., 2011), again highlighting the complexity of intestinal homeostasis and a need for further research.

Taken together, this work highlights the double-edged sword of host adaptation to dysbiosis, in which, under dysbiotic conditions like psoriasis, $CX_3CR_1^{hi}$ macrophages may proliferate to maintain gut homeostasis, with the risk of aggravating gut inflammation when environmental challenges are encountered. This finding may explain why patients with psoriasis, having enriched colonic TNF, are at high risk of developing IBD.

Strategies aiming at restoring a healthy gut microbiota in psoriasis would thus prevent the development of comorbidities such as IBD. This work also emphasizes the need for a holistic rather than palliative approach to disease treatment for long-term benefits to health.

Figure 6. IMQ-induced psoriasis predisposes mice to exacerbated DSS colitis

(A–E) Colonic *Tnf* (A), *Il10* (B), *Tgfb* (C), *Ifng* (D), and *Il22* (E) gene expression normalized to the housekeeping gene *Rpl13a* assessed by qPCR in mock- versus daily 2 mg imiquimod-treated mice (IMQ-pso) after 6 days. Data are presented as a fold change relative to expression in mock-treated mice (n = 5–10 biological replicates/group).

(F) Gene set enrichment analysis showing enrichment of TNFα signaling via NF-κB gene set in the transcriptome data of sigmoidal colonic biopsy samples from psoriasis patients compared with healthy controls.

(G and H) HEK-TLR reporter cells were incubated for 5 h with suspended feces supernatant (1:100 dilution) from control versus IMQ-pso mice to quantify the relative concentration of TLR2 ligand (G) and TLR4 ligand (H) through colorimetric assay readout (OD at 630 nm) (n = 5–6 biological replicates/group).

(I) Gene set enrichment analysis showing enrichment of inflammatory response in the transcriptome data of sigmoidal colonic biopsy samples from psoriasis patients compared with healthy controls.

(J and K) Colon length (J) and proportion of colonic lamina propria $Ly6C^{hi}$ monocytes among $CD45^+$ (K) in mock-treated mice versus mice treated daily for 6 days with 2 mg imiquimod (IMQ-pso) (n = 5–14 biological replicates/group).

(L) Colonic *Mmp7* expression normalized to *Rpl13a* assessed by qPCR in mock- versus imiquimod-treated mice (IMQ-pso) after 6 days. Data are presented as a fold change relative to mock-treated mice (n = 12–15 biological replicates/group).

(M–Q) Mice were treated for 4 days with 2 mg imiquimod (IMQ-pso +) or mock treated (IMQ-pso −) and then their water was supplemented with 3% DSS (+) or not (−) for 5 days as indicated in the timeline (M). Clinical scores (N) and weights (O) were analyzed over 5 days on DSS treatment, and colon length was measured and expressed relative to non-DSS control at the endpoint (day 9) (P). Colonic inflammation was assessed by histological scoring of H&E-stained colonic sections from colon collected at the endpoint (Q, right) and representative H&E-stained colonic sections are shown (Q, left): top left, water-mock-treated mice; top right, water + IMQ-pso; bottom left, DSS + mock; bottom right, DSS + IMQ-pso (n = 4–8 biological replicates/group). Results are shown as the mean ± SEM. *$p < 0.05$, **$p < 0.005$ by Mann-Whitney U test where two groups are present and Kruskal-Wallis test where three or more groups are present. See also Figures S5 and S6.

Limitations of the study

The first limitation of our study is that it was done in experimental mice and a validation in humans would be necessary to conclude that psoriasis promotes the proliferation of colonic $CX_3CR_1^{hi}$ macrophages in humans and increases susceptibility to IBD. Furthermore, while we have demonstrated that IMQ-pso resulted in gut microbiota dysbiosis, we found that IL-17 on its own was not the causative factor. Thus, a more extensive study would be necessary to identify which factors trigger dysbiosis, which would be insightful in psoriasis but also in most chronic diseases. Finally, how succinate promoted $CX_3CR_1^{hi}$ macrophage proliferation has not been identified here. Further investigations, while outside of the scope of this study, would add value to our findings.

STAR★METHODS

Detailed methods are provided in the online version of this paper and include the following:

- KEY RESOURCES TABLE
- RESOURCE AVAILABILITY
  - Lead contact
  - Materials availability
  - Data and code availability
- EXPERIMENTAL MODEL AND SUBJECT DETAILS
  - Mice
  - HEK 293 cell lines
- METHOD DETAILS
  - Germ free mouse microbial recolonisation
  - Imiquimod-induced psoriasis induction
  - Administration of immune modifying particles (IMP)
  - DSS colitis model and scoring
  - BrdU staining for flow cytometry
  - IL-17 administration
  - Flow cytometry
  - Histology and dermal measurements
  - Bacteria 16S rRNA gene amplicon sequencing and bioinformatics
  - Bacterial metabolite analysis using nuclear magnetic resonance (NMR) spectroscopy
  - RNA extraction and real Time PCR
  - Colon *ex vivo* cell culture
- QUANTIFICATION AND STATISTICAL ANALYSIS
  - Statistics

16/j.

ACKNOWLEDGMENTS

G.P. and D.N. are recipients of the Australian Government Research Training Program Scholarship, and L.M. and J.K.T. are a'Beckett fellows. This work was supported by the Australian Research Council Linkage grant 160100627 cofunded by Sanitarium. The authors would like to acknowledge Sydney Cytometry for support in flow cytometry as well as staff from the CPC animal facility. The graphical abstract was created with BioRender (BioRender.com).

AUTHOR CONTRIBUTIONS

G.V.P., J.K.T., and L.M. designed the project, did the experiments, and wrote the manuscript. L.M. and S.J.S. funded the project. J.K.T. did the microbiota analysis. G.V.P., J.K.T., and L.M. analyzed and curated data. D.N., J.T., C.I.D, and J.M. participated in the experiments. R.J.M. and D.S. participated in the microbiota study. S.S. and N.K. helped with the study design and with the manuscript writing.

DECLARATION OF INTERESTS

The authors declare no competing interests.

REFERENCES

Armstrong, H., Mander, I., Zhang, Z., Armstrong, D., and Wine, E. (2021). Not all fibers are born equal; variable response to dietary fiber subtypes in IBD. Front. Pediatr. *8*, 620189. https://www.frontiersin.org/article/10.3389/fped.2020.620189.

Bain, C.C., and Schridde, A. (2018). Origin, differentiation, and function of intestinal macrophages. Front. Immunol. *9*, 2733. https://doi.org/10.3389/fimmu.2018.02733.

Bain, C.C., Scott, C.L., and Mowat, A.M. (2012). Resident and pro-inflammatory macrophages in the colon represent alternative context dependent fates of the same Ly6Chi monocyte precursors. Immunology *137*, 218.

Balato, N., Napolitano, M., Ayala, F., Patruno, C., Megna, M., and Tarantino, G. (2015). Nonalcoholic fatty liver disease, spleen and psoriasis: new aspects of low-grade chronic inflammation. World J. Gastroenterol. *21*, 6892–6897. https://doi.org/10.3748/wjg.v21.i22.6892.

Bhaskaran, N., Quigley, C., Paw, C., Butala, S., Schneider, E., and Pandiyan, P. (2018). Role of short chain fatty acids in controlling tregs and immunopathology during mucosal infection. Front. Microbiol. *9*, 1995. https://doi.org/10.3389/fmicb.2018.01995.

Brembilla, N.C., Senra, L., and Boehncke, W.H. (2018). The IL-17 family of cytokines in psoriasis: IL-17A and beyond. Front. Immunol. *9*, 1682. https://doi.org/10.3389/fimmu.2018.01682.

Cai, Y., Shen, X., Ding, C., Qi, C., Li, K., Li, X., Jala, V.R., Zhang, H.g., Wang, T., Zheng, J., and Yan, J. (2011). Pivotal role of dermal IL-17-producing gamma delta T cells in skin inflammation. Immunity *35*, 596–610. https://doi.org/10.1016/j.immuni.2011.08.001.

Callahan, B. (2017). RDP taxonomic training data formatted for DADA2 (RDP trainset 16/release 11.5). Zenodo. https://doi.org/10.5281/zenodo.801828.

Callahan, B.J., McMurdie, P.J., Rosen, M.J., Han, A.W., Johnson, A.J.A., and Holmes, S.P. (2016). DADA2: high-resolution sample inference from Illumina amplicon data. Nat. Methods *13*, 581–583. https://doi.org/10.1038/nmeth.3869.

Chang, H.-W. Yan D., Singh R., Bui A., Lee K.M., Truong A., Milush J.M., Somsouk M., Liao W. (2021) Metagenomic analysis of the gut microbiome in psoriasis reveals three subgroups with distinct host-microbe interactions. Available at Research Square. https://doi.org/10.21203/rs.3.rs-58641/v1.

de Castro Fonseca, M., Aguiar, C.J., da Rocha Franco, J.A., Gingold, R.N., and Leite, M.F. (2016). GPR91: expanding the frontiers of Krebs cycle intermediates. Cell Commun. Signal. *14*, 3. https://doi.org/10.1186/s12964-016-0126-1.

Di Cesare, A., Di Meglio, P., and Nestle, F.O. (2009). The IL-23/Th17 Axis in the immunopathogenesis of psoriasis. J. Invest. Dermatol. *129*, 1339–1350. https://doi.org/10.1038/jid.2009.59.

Chandran, V., and Raychaudhuri, S.P. (2010). Geoepidemiology and environmental factors of psoriasis and psoriatic arthritis. J. Autoimmun. *34*, J314–J321. https://doi.org/10.1016/j.jaut.2009.12.001.

Chen, S., Han, K., Li, H., Cen, J., Yang, Y., Wu, H., and Wei, Q. (2017a). Isogarcinol extracted from Garcinia mangostana L. Ameliorates imiquimod-induced psoriasis -like skin lesions in mice. J. Agric. Food Chem. *65*, 846–857. https://doi.org/10.1021/acs.jafc.6b05207.

Chen, Y.-H., Wu, C.S., Chao, Y.H., Lin, C.C., Tsai, H.Y., Li, Y.R., Chen, Y.Z., Tsai, W.H., and Chen, Y.K. (2017b). Lactobacillus pentosus GMNL-77 inhibits skin lesions in imiquimod-induced psoriasis-like mice. J. Food Drug Anal. *25*, 559–566. https://doi.org/10.1016/j.jfda.2016.06.003.

Christophers, E. (2001). Psoriasis–epidemiology and clinical spectrum. Clin. Exp. Dermatol. *26*, 314–320. https://doi.org/10.1046/j.1365-2230.2001.00832.x.

Codoner, F.M., Ramírez-Bosca, A., Climent, E., Carrión-Gutierrez, M., Guerrero, M., Pérez-Orquín, J.M., Horga de la Parte, J., Genovés, S., Ramón, D., Navarro-López, V., and Chenoll, E. (2018). Gut microbial composition in patients with psoriasis. Sci. Rep. *8*, 3812. https://doi.org/10.1038/s41598-018-22125-y.

Connors, J., Dawe, N., and Van Limbergen, J. (2018). The role of succinate in the regulation of intestinal inflammation. Nutrients *11*, 25. https://doi.org/10.3390/nu11010025.

Cossarizza, A., Chang, H., Radbruch, A., Acs, A., Adam, D., Adam-Klages, S., Agace, W.W., Aghaeepour, N., Akdis, M., Allez, M., et al. (2019). Guidelines for the use of flow cytometry and cell sorting in immunological studies (second edition). Eur. J. Immunol. *49*, 1457–1973. https://doi.org/10.1002/eji.201970107.

Cottone, M., Sapienza, C., Macaluso, F.S., and Cannizzaro, M. (2019). Psoriasis and inflammatory bowel disease. Dig. Dis. *37*, 451–457. https://doi.org/10.1159/000500116.

Derkacz, A., Olczyk, P., Olczyk, K., and Komosinska-Vassev, K. (2021). The role of extracellular matrix components in inflammatory bowel diseases. J. Clin. Med. *10*, 1122. https://doi.org/10.3390/jcm10051122.

Desalegn, G., and Pabst, O. (2019). Inflammation triggers immediate rather than progressive changes in monocyte differentiation in the small intestine. Nat. Commun. *10*, 3229. https://doi.org/10.1038/s41467-019-11148-2.

Dogra, S., and Mahajan, R. (2016). Psoriasis: epidemiology, clinical features, co-morbidities, and clinical scoring. Indian Dermatol. Online J. *7*, 471–480. https://doi.org/10.4103/2229-5178.193906.

Erridge, C., Duncan, S.H., Bereswill, S., and Heimesaat, M.M. (2010). The induction of colitis and ileitis in mice is associated with marked increases in intestinal concentrations of stimulants of TLRs 2, 4, and 5. PLoS One *5*, e9125. https://doi.org/10.1371/journal.pone.0009125.

Fernandez-Veledo, S., and Vendrell, J. (2019). Gut microbiota-derived succinate: friend or foe in human metabolic diseases? Rev. Endocr. Metab. Disord. *20*, 439–447. https://doi.org/10.1007/s11154-019-09513-z.

van der Fits, L., Mourits, S., Voerman, J.S.A., Kant, M., Boon, L., Laman, J.D., Cornelissen, F., Mus, A.M., Florencia, E., Prens, E.P., and Lubberts, E. (2009). Imiquimod-induced psoriasis-like skin inflammation in mice is mediated via the IL-23/IL-17 Axis. J. Immunol. *182*, 5836–5845. https://doi.org/10.4049/jimmunol.0802999.

Fitz, L., Zhang, W., Soderstrom, C., Fraser, S., Lee, J., Quazi, A., Wolk, R., Mebus, C.A., Valdez, H., and Berstein, G. (2018). Association between serum interleukin-17A and clinical response to tofacitinib and etanercept in moderate to severe psoriasis. Clin. Exp. Dermatol. *43*, 790–797. https://doi.org/10.1111/ced.13561.

Fremder, M., Kim, S.W., Khamaysi, A., Shimshilashvili, L., Eini-Rider, H., Park, I.S., Hadad, U., Cheon, J.H., and Ohana, E. (2021). A transepithelial pathway delivers succinate to macrophages, thus perpetuating their pro-inflammatory metabolic state. Cell Rep. *36*, 109521. https://doi.org/10.1016/j.celrep.2021.109521.

Furusawa, Y., Obata, Y., Fukuda, S., Endo, T.A., Nakato, G., Takahashi, D., Nakanishi, Y., Uetake, C., Kato, K., Kato, T., et al. (2014). Commensal microbe-derived butyrate induces the differentiation of colonic regulatory T cells (vol 504, pg 446, 2013). Nature, 254. https://doi.org/10.1038/nature13041.

Getts, D.R., Terry, R.L., Getts, M.T., Deffrasnes, C., Müller, M., van Vreden, C., Ashhurst, T.M., Chami, B., McCarthy, D., Wu, H., et al. (2014). Therapeutic inflammatory monocyte modulation using immune-modifying microparticles. Sci. Transl. Med. *6*, 219ra7. https://doi.org/10.1126/scitranslmed.3007563.

Gloor, G.B., Macklaim, J.M., Pawlowsky-Glahn, V., and Egozcue, J.J. (2017). Microbiome datasets are compositional: and this is not optional. Front. Microbiol. *8*, 2224. https://doi.org/10.3389/fmicb.2017.02224.

Grine, L., Steeland, S., Van Ryckeghem, S., Ballegeer, M., Lienenklaus, S., Weiss, S., Sanders, N.N., Vandenbroucke, R.E., and Libert, C. (2016). Topical imiquimod yields systemic effects due to unintended oral uptake. Sci. Rep. *6*, 20134. https://doi.org/10.1038/srep20134.

Groeger, D., O'Mahony, L., Murphy, E.F., Bourke, J.F., Dinan, T.G., Kiely, B., Shanahan, F., and Quigley, E.M.M. (2013). Bifidobacterium infantis 35624 modulates host inflammatory processes beyond the gut. Gut Microb. *4*, 325–339. https://doi.org/10.4161/gmic.25487.

Han, X., Ding, S., Jiang, H., and Liu, G. (2021). Roles of macrophages in the development and treatment of gut inflammation. Front. Cell Dev. Biol. *9*, 625423. https://doi.org/10.3389/fcell.2021.625423.

Hanauer, S.B., Feagan, B.G., Lichtenstein, G.R., Mayer, L.F., Schreiber, S., Colombel, J.F., Rachmilewitz, D., Wolf, D.C., Olson, A., Bao, W., et al. (2002). Maintenance infliximab for Crohn's disease: the ACCENT I randomised trial. Lancet *359*, 1541–1549. https://doi.org/10.1016/S0140-6736(02)08512-4.

Hayden, D.M., Forsyth, C., and Keshavarzian, A. (2011). The role of matrix metalloproteinases in intestinal epithelial wound healing during normal and inflammatory states. J. Surg. Res. *168*, 315–324. https://doi.org/10.1016/j.jss.2010.03.002.

He, J., Song, Y., Li, G., Xiao, P., Liu, Y., Xue, Y., Cao, Q., Tu, X., Pan, T., Jiang, Z., et al. (2019). Fbxw7 increases CCL2/7 in CX3CR1hi macrophages to promote intestinal inflammation. J. Clin. Invest. *129*, 3877–3893. https://doi.org/10.1172/JCI123374.

Kimball, A.B., Gladman, D., Gelfand, J.M., Gordon, K., Horn, E.J., Korman, N.J., Korver, G., Krueger, G.G., Strober, B.E., and Lebwohl, M.G.; National Psoriasis Foundation (2008). National Psoriasis Foundation clinical consensus on psoriasis comorbidities and recommendations for screening. J. Am. Acad. Dermatol. *58*, 1031–1042. https://doi.org/10.1016/j.jaad.2008.01.006.

Koscsó, B., Kurapati, S., Rodrigues, R.R., Nedjic, J., Gowda, K., Shin, C., Soni, C., Ashraf, A.Z., Purushothaman, I., Palisoc, M., et al. (2020). Gut-resident CX3CR1hi macrophages induce tertiary lymphoid structures and IgA response in situ. Sci. Immunol. *5*, eaax0062. https://doi.org/10.1126/sciimmunol.aax0062.

Kostadinova, F.I., Baba, T., Ishida, Y., Kondo, T., Popivanova, B.K., and Mukaida, N. (2010). Crucial involvement of the CX3CR1-CX3CL1 axis in dextran sulfate sodium-mediated acute colitis in mice. J. Leukoc. Biol. *88*, 133–143. https://doi.org/10.1189/jlb.1109768.

Lazar, V., Ditu, L.M., Pircalabioru, G.G., Gheorghe, I., Curutiu, C., Holban, A.M., Picu, A., Petcu, L., and Chifiriuc, M.C. (2018). Aspects of gut microbiota and immune system interactions in infectious diseases, immunopathology, and cancer. Front. Immunol. *9*, 1830. https://doi.org/10.3389/fimmu.2018.01830.

Li, W.Q., Han, J.L., Chan, A.T., and Qureshi, A.A. (2013). Psoriasis, psoriatic arthritis and increased risk of incident Crohn's disease in US women. Ann. Rheum. Dis. *72*, 1200–1205. https://doi.org/10.1136/annrheumdis-2012-202143.

Littlewood-Evans, A., Sarret, S., Apfel, V., Loesle, P., Dawson, J., Zhang, J., Muller, A., Tigani, B., Kneuer, R., Patel, S., et al. (2016). GPR91 senses extracellular succinate released from inflammatory macrophages and exacerbates rheumatoid arthritis. J. Exp. Med. *213*, 1655–1662. https://doi.org/10.1084/jem.20160061.

Macia, L., Tan, J., Vieira, A.T., Leach, K., Stanley, D., Luong, S., Maruya, M., Ian McKenzie, C., Hijikata, A., Wong, C., et al. (2015). Metabolite-sensing receptors GPR43 and GPR109A facilitate dietary fibre-induced gut homeostasis through regulation of the inflammasome. Nat. Commun. *6*, 6734. https://doi.org/10.1038/ncomms7734.

Mao, H., Yang, A., Zhao, Y., Lei, L., and Li, H. (2020). Succinate supplement elicited "Pseudohypoxia" condition to promote proliferation, migration, and osteogenesis of periodontal ligament cells. Stem Cells Int. *2020*, 2016809. https://doi.org/10.1155/2020/2016809.

Medina-Contreras, O., Geem, D., Laur, O., Williams, I.R., Lira, S.A., Nusrat, A., Parkos, C.A., and Denning, T.L. (2011). CX3CR1 regulates intestinal macrophage homeostasis, bacterial translocation, and colitogenic Th17 responses in mice. J. Clin. Invest. *121*, 4787–4795. https://doi.org/10.1172/Jci59150.

Miller, I., Min, M., Yang, C., Tian, C., Gookin, S., Carter, D., and Spencer, S.L. (2018). Ki67 is a graded rather than a binary marker of proliferation versus quiescence. Cell Rep. *24*, 1105–1112.e5. https://doi.org/10.1016/j.celrep.2018.06.110.

Morita, N., Umemoto, E., Fujita, S., Hayashi, A., Kikuta, J., Kimura, I., Haneda, T., Imai, T., Inoue, A., Mimuro, H., et al. (2019). GPR31-dependent dendrite protrusion of intestinal CX3CR1(+) cells by bacterial metabolites. Nature *566*, 110–114. https://doi.org/10.1038/s41586-019-0884-1.

Muzes, G., Molnár, B., Tulassay, Z., and Sipos, F. (2012). Changes of the cytokine profile in inflammatory bowel diseases. World J. Gastroenterol. *18*, 5848–5861. https://doi.org/10.3748/wjg.v18.i41.5848.

Na, Y.R., Stakenborg, M., Seok, S.H., and Matteoli, G. (2019). Macrophages in intestinal inflammation and resolution: a potential therapeutic target in IBD. Nat. Rev. Gastroenterol. Hepatol. *16*, 531–543. https://doi.org/10.1038/s41575-019-0172-4.

Nastasi, C., Candela, M., Bonefeld, C.M., Geisler, C., Hansen, M., Krejsgaard, T., Biagi, E., Andersen, M.H., Brigidi, P., Ødum, N., et al. (2015). The effect of short-chain fatty acids on human monocyte-derived dendritic cells. Sci. Rep. *5*, 16148. https://doi.org/10.1038/srep16148.

Neimann, A.L., Shin, D.B., Wang, X., Margolis, D.J., Troxel, A.B., and Gelfand, J.M. (2006). Prevalence of cardiovascular risk factors in patients with psoriasis. J. Am. Acad. Dermatol. *55*, 829–835. https://doi.org/10.1016/j.jaad.2006.08.040.

de Oliveira, M.d.F., Rocha, B.d.O., and Duarte, G.V. (2015). Psoriasis: classical and emerging comorbidities. An. Bras. Dermatol. *90*, 9–20. https://doi.org/10.1590/abd1806-4841.20153038.

Parisi, R., Symmons, D.P.M., Griffiths, C.E.M., and Ashcroft, D.M.; Identification and Management of Psoriasis and Associated ComorbidiTy IMPACT project team (2013). Global epidemiology of psoriasis: a systematic review of incidence and prevalence. J. Invest. Dermatol. *133*, 377–385. https://doi.org/10.1038/jid.2012.339.

Pinget, G.V., Tan, J., Niewold, P., Mazur, E., Angelatos, A.S., King, N.J.C., and Macia, L. (2020). Immune modulation of monocytes dampens the IL-17(+) gammadelta T cell response and associated psoriasis pathology in mice. J. Invest. Dermatol. *140*, 2398–2407.e1. https://doi.org/10.1016/j.jid.2020.03.973.

Rohm, T.V., Fuchs, R., Müller, R.L., Keller, L., Baumann, Z., Bosch, A.J.T., Schneider, R., Labes, D., Langer, I., Pilz, J.B., et al. (2021). Obesity in humans is characterized by gut inflammation as shown by pro-inflammatory intestinal macrophage accumulation. Front. Immunol. *12*, 668654. https://www.frontiersin.org/article/10.3389/fimmu.2021.668654.

Rohm, T.V., Keller, L., Bosch, A.J.T., AlAsfoor, S., Baumann, Z., Thomas, A., Wiedemann, S.J., Steiger, L., Dalmas, E., Wehner, J., et al. (2022). Targeting colonic macrophages improves glycemic control in high-fat diet-induced obesity. Commun. Biol. *5*, 370. https://doi.org/10.1038/s42003-022-03305-z.

Scher, J.U., Ubeda, C., Artacho, A., Attur, M., Isaac, S., Reddy, S.M., Marmon, S., Neimann, A., Brusca, S., Patel, T., et al. (2015). Decreased bacterial diversity characterizes the altered gut microbiota in patients with psoriatic arthritis, resembling dysbiosis in inflammatory bowel disease. Arthritis Rheumatol. *67*, 128–139. https://doi.org/10.1002/art.38892.

Schneider, K.M., Bieghs, V., Heymann, F., Hu, W., Dreymueller, D., Liao, L., Frissen, M., Ludwig, A., Gassler, N., Pabst, O., et al. (2015). CX3CR1 is a gatekeeper for intestinal barrier integrity in mice: limiting steatohepatitis by maintaining intestinal homeostasis. Hepatology *62*, 1405–1416. https://doi.org/10.1002/hep.27982.

Schulthess, J., Pandey, S., Capitani, M., Rue-Albrecht, K.C., Arnold, I., Franchini, F., Chomka, A., Ilott, N.E., Johnston, D.G.W., Pires, E., et al. (2019). The short chain fatty acid butyrate imprints an antimicrobial Program in macrophages. Immunity *50*, 432–445.e7. https://doi.org/10.1016/j.immuni.2018.12.018.

Schwarzenberger, P., La Russa, V., Miller, A., Ye, P., Huang, W., Zieske, A., Nelson, S., Bagby, G.J., Stoltz, D., Mynatt, R.L., et al. (1998). IL-17 stimulates granulopoiesis in mice: use of an alternate, novel gene therapy-derived method for in vivo evaluation of cytokines. J. Immunol. *161*, 6383–6389.

Shaw, T.N., Houston, S.A., Wemyss, K., Bridgeman, H.M., Barbera, T.A., Zangerle-Murray, T., Strangward, P., Ridley, A.J.L., Wang, P., Tamoutounour, S., et al. (2018). Tissue-resident macrophages in the intestine are long lived and defined by Tim-4 and CD4 expression. J. Exp. Med. *215*, 1507–1518. https://doi.org/10.1084/jem.20180019.

Shinno-Hashimoto, H., Hashimoto, Y., Wei, Y., Chang, L., Fujita, Y., Ishima, T., Matsue, H., and Hashimoto, K. (2021). Abnormal composition of microbiota in the gut and skin of imiquimod-treated mice. Sci. Rep. *11*, 11265. https://doi.org/10.1038/s41598-021-90480-4.

Sikora, M., Chrabąszcz, M., Maciejewski, C., Zaremba, M., Waśkiel, A., Olszewska, M., and Rudnicka, L. (2018). Intestinal barrier integrity in patients with plaque psoriasis. J. Dermatol. *45*, 1468–1470. https://doi.org/10.1111/1346-8138.14647.

Steinbach, E.C., and Plevy, S.E. (2014). The role of macrophages and dendritic cells in the initiation of inflammation in IBD. Inflamm. Bowel Dis. *20*, 166–175. https://doi.org/10.1097/MIB.0b013e3182a69dca.

Stoppelenburg, A.J., Salimi, V., Hennus, M., Plantinga, M., Huis in 't Veld, R., Walk, J., Meerding, J., Coenjaerts, F., Bont, L., and Boes, M. (2013). Local IL-17A potentiates early neutrophil recruitment to the respiratory tract during severe RSV infection. PLoS One *8*, e78461. https://doi.org/10.1371/journal.pone.0078461.

Subramanian, A., Tamayo, P., Mootha, V.K., Mukherjee, S., Ebert, B.L., Gillette, M.A., Paulovich, A., Pomeroy, S.L., Golub, T.R., Lander, E.S., and Mesirov, J.P. (2005). Gene set enrichment analysis: a knowledge-based approach for interpreting genome-wide expression profiles. Proc. Natl. Acad. Sci. USA *102*, 15545–15550. https://doi.org/10.1073/pnas.0506580102.

Takuathung, M.N., Wongnoppavich, A., Panthong, A., Khonsung, P., Chiranthanut, N., Soonthornchareonnon, N., and Sireeratawong, S. (2018). Antipsoriatic effects of wannachawee recipe on imiquimod-induced psoriasis-like dermatitis in BALB/c mice. Evid. Base Compl. Alternative Med., 7931031. https://doi.org/10.1155/2018/7931031.

Tan, J., McKenzie, C., Potamitis, M., Thorburn, A.N., Mackay, C.R., and Macia, L. (2014). The role of short-chain fatty acids in health and disease. Adv. Immunol. *121*, 91–119. https://doi.org/10.1016/B978-0-12-800100-4.00003-9.

Tan, J., McKenzie, C., Vuillermin, P.J., Goverse, G., Vinuesa, C.G., Mebius, R.E., Macia, L., and Mackay, C.R. (2016). Dietary fiber and bacterial SCFA enhance oral tolerance and protect against food allergy through diverse cellular pathways. Cell Rep. *15*, 2809–2824. https://doi.org/10.1016/j.celrep.2016.05.047.

Tan, J., Ni, D., Taitz, J., Pinget, G.V., Read, M., Senior, A., Wali, J.A., Elnour, R., Shanahan, E., Wu, H., et al. (2022). Dietary protein increases T cell independent sIgA production through changes in gut microbiota-derived extracellular vesicles. Nat. Commun. *13*, 4336. https://doi.org/10.1038/s41467-022-31761-y.

Tan, L., Zhao, S., Zhu, W., Wu, L., Li, J., Shen, M., Lei, L., Chen, X., and Peng, C. (2018). The Akkermansia muciniphila is a gut microbiota signature in psoriasis. Exp. Dermatol. *27*, 144–149. https://doi.org/10.1111/exd.13463.

Tan, J., Ni, D., Ribeiro, R.V., Pinget, G.V., and Macia, L. (2021). How changes in the nutritional landscape shape gut immunometabolism. Nutrients *13*, 823. https://doi.org/10.3390/nu13030823.

Tannahill, G.M., Curtis, A.M., Adamik, J., Palsson-McDermott, E.M., McGettrick, A.F., Goel, G., Frezza, C., Bernard, N.J., Kelly, B., Foley, N.H., et al. (2013). Succinate is an inflammatory signal that induces IL-1 beta through HIF-1 alpha. Nature *496*, 238–242. https://doi.org/10.1038/nature11986.

Visser, M.J.E., Kell, D.B., and Pretorius, E. (2019). Bacterial dysbiosis and translocation in psoriasis vulgaris. Front. Cell. Infect. Microbiol. *9*, 7. https://doi.org/10.3389/fcimb.2019.00007.

van der Voort, E.A.M., Koehler, E.M., Dowlatshahi, E.A., Hofman, A., Stricker, B.H., Janssen, H.L.A., Schouten, J.N.L., and Nijsten, T. (2014). Psoriasis is independently associated with nonalcoholic fatty liver disease in patients 55 years old or older: results from a population-based study. J. Am. Acad. Dermatol. *70*, 517–524. https://doi.org/10.1016/j.jaad.2013.10.044.

Xu, J., Duan, X., Hu, F., Poorun, D., Liu, X., Wang, X., Zhang, S., Gan, L., He, M., Zhu, K., et al. (2018). Resolvin D1 attenuates imiquimod-induced mice psoriasiform dermatitis through MAPKs and NF-kappa B pathways. J. Dermatol. Sci. *89*, 127–135. https://doi.org/10.1016/j.jdermsci.2017.10.016.

Yang, R., Zhou, Q., Wen, C., Hu, J., Li, H., Zhao, M., and Zhao, H. (2013). Mustard seed (Sinapis Alba Linn) attenuates imiquimod-induced psoriasiform inflammation of BALB/c mice. J. Dermatol. *40*, 543–552. https://doi.org/10.1111/1346-8138.12119.

Zakostelska, Z., Málková, J., Klimešová, K., Rossmann, P., Hornová, M., Novosádová, I., Stehlíková, Z., Kostovčík, M., Hudcovic, T., Štepánková, R., et al. (2016). Intestinal microbiota promotes psoriasis-like skin inflammation by enhancing Th17 response. PLoS One *11*, e0159539. https://doi.org/10.1371/journal.pone.0159539.

Zeitouni, N.E., Chotikatum, S., von Köckritz-Blickwede, M., and Naim, H.Y. (2016). The impact of hypoxia on intestinal epithelial cell functions: consequences for invasion by bacterial pathogens. Mol. Cell. Pediatr. *3*, 14. https://doi.org/10.1186/s40348-016-0041-y.

Zigmond, E., Bernshtein, B., Friedlander, G., Walker, C.R., Yona, S., Kim, K.W., Brenner, O., Krauthgamer, R., Varol, C., Müller, W., and Jung, S. (2014). Macrophage-restricted interleukin-10 receptor deficiency, but not IL-10 deficiency, causes severe spontaneous colitis. Immunity *40*, 720–733. https://doi.org/10.1016/j.immuni.2014.03.012.

STAR★METHODS

KEY RESOURCES TABLE

REAGENT or RESOURCE	SOURCE	IDENTIFIER
Antibodies		
Anti-mouse CD103 PerCP/Cyanine5.5 (Clone 2E7)	BioLegend	Cat#121416; RRID:AB_2128621
Anti-mouse CD11c FITC (Clone N418)	BioLegend	Cat#117306; RRID:AB_313775
Anti-mouse CD3 AF488 (Clone 17A2)	BioLegend	Cat#100210; RRID:AB_389301
Anti-mouse CD4 PerCP/Cy5.5 (Clone GK1.5)	BioLegend	Cat#100434; RRID:AB_893324
Anti-mouse CD45 BV785 (Clone 30-F11)	BioLegend	Cat#103149; RRID:AB_2564590
Anti-mouse CD64 PE/Cy7 (Clone X54-5/7.1)	BioLegend	Cat#139314; RRID:AB_2563904
Anti-mouse CD8a BV650 (Clone 53-6.7)	BioLegend	Cat#100742; RRID:AB_2563056
Anti-mouse CX3CR1 PE (Clone SA011F11)	BioLegend	Cat#149006; RRID:AB_2564315
Anti-mouse F4/80 PE/Cy7 (Clone BM8)	BioLegend	Cat#123114; RRID:AB_893478
Anti-mouse I-Ab Pacific Blue (Clone AF6-120.1)	BioLegend	Cat#116422; RRID:AB_10613473
Anti-mouse Ki67 AF488 (Clone 16A8)	BioLegend	Cat#652418; RRID:AB_2564269
Anti-mouse Ly6C BV605 (Clone HK1.4)	BioLegend	Cat#128036; RRID:AB_2562353
Anti-mouse CD49b PE/Cy7 (Clone DX5)	BioLegend	Cat#108922; RRID:AB_2561460
Anti-mouse Ly6G AF647 (Clone 1A8)	BioLegend	Cat#127610; RRID:AB_1134159
Anti-mouse CD16/32 (Clone 93)	BioLegend	Cat#101320;RRID:AB_1574975
Anti-mouse CD11b BUV395 (Clone M1/70)	BD	Cat#563553; RRID:AB_1134159
Anti-mouse CD24 BUV737 (Clone M1/69)	BD	Cat#565308; RRID:AB_2739174
Anti-mouse IL-17A PE (Clone REA660)	Miltenyi	Cat#130-112-009; RRID: AB_2652360
Anti-mouse Gamma delta TCR (Clone GL3)	eBioscience	Cat#15-5711-82; RRID: AB_468804
Chemicals, peptides, and recombinant proteins		
PBS	Thermo Fisher Scientific	Cat#18912014
Adlara (Imiquimod)	iNova Pharmaceuticals	Cat#1643032
Veet Pure Hair Removal Cream Legs and Body Sensitive Skin	Veet	Cat#EA_3019439
Immune Modifying Particles poly(lactic-co-glycolic acid)	Phosphorex Inc	Cat#LG500
Dextran sulfate sodium salt	MP Biomedical	Cat#216011050
Recombinant IL-17A/F	BioLegend	Cat#580804
Foetal Bovine Serum	Bovogen Biologicals	Cat#AFBS-500
HBSS	Thermo Fisher Scientific	Cat#24020117
RPMI	Thermo Fisher Scientific	Cat#21870092
Penicillin/Streptomycin	Sigma-Aldrich	Cat#15140122
HEPES	Thermo Fisher Scientific	Cat#15630080
Collagenase type IV	Thermo Fisher Scientific	Cat#17104019
Percoll	Cytiva	Cat#17089101
L-Glutamine	Sigma-Aldrich	Cat#G7513
Phorbol 12-myristate 13-acetate	Sigma-Aldrich	Cat#P8139
Ionomycin calcium salt from Streptomyces conglobatus	Sigma-Aldrich	Cat#I0634
Brefeldin A	BioLegend	Cat#420601
Deuterium oxide	Sigma-Aldrich	Cat#151882
Deuterium methanol	Sigma-Aldrich	Cat#151947
Deuterium chloroform	Sigma-Aldrich	Cat#151823

(*Continued on next page*)

Continued

REAGENT or RESOURCE	SOURCE	IDENTIFIER
4,4-dimethyl-4-silapentane-1-sulfonic acid	Sigma-Aldrich	Cat#178837
TRI Reagent	Sigma-Aldrich	Cat#T9424
iScript™ Reverse Transcription Supermix for RT-qPCR	BioRad	Cat#1708841
SYBR Green	BioRad	Cat#1725121
Sodium succinate	Sigma-Aldrich	Cat#S2378
Critical commercial assays		
BrdU staining kit	BD	Cat#552598
Fixation/Permeabilization Solution Kit	BD	Cat#554714
FastDNA Spin Kit for Feces	MP Biomedicals	Cat#116570200
LIVE/DEAD™ Fixable Blue Dead Cell Stain Kit, for UV excitation	Thermo Fisher Scientific	Cat#L34962
Deposited data		
16S rRNA sequencing data	This paper	Accession: PRJEB47653
RNAseq transcriptome data from sigmoidal gut biopsy	(Chang et al., 2021)	Accession: GSE150851
Experimental models: Cell lines		
HEK-Blue mTLR2 murine TLR2 reporter HEK293 cells	InvivoGen	Cat#hkb-mtlr2
HEK-Blue mTLR4 murine TLR4 reporter HEK293 cells	InvivoGen	Cat#hkb-mtlr4
Experimental models: Organisms/strains		
Mus muculus (C57BL/6)	Australian BioResources	JAX:000664
Oligonucleotides		
See Table S1	Sigma-Aldrich	N/A
Software and algorithms		
Graphpad Prism v10	GraphPad Software	RRID:SCR_008520
R Project for Statistical Computing 3.6.1	R Foundation	RRID:SCR_001905
RStudio 1.3.1093	RStudio	RRID:SCR_000432
Gene Set Enrichment Analysis	Broad Institute	RRID:SCR_003199
FlowJo v10	FlowJo Inc.	RRID:SCR_008520
ImageJ	National Institutes of Health	RRID:SCR_003070
Adobe Illustrator 2022	Adobe	RRID:SCR_010279
Other		
Mouse diet – AIN93G normal chow	Specialty Feeds	Cat#AIN93G
Mouse Elizabethan collar	Able Scientific	Cat#ASMCE1GM

RESOURCE AVAILABILITY

Lead contact

Further information and requests for resources and reagents should be directed to and will be fulfilled by the lead contact, Laurence Macia (Laurence.macia@sydney.edu.au).

Materials availability

This study did not generate new unique reagents.

Data and code availability

16S rRNA gene amplicon sequencing data have been deposited at European Nucleotide Archive and are publicly available as of the date of publication. Accession numbers are listed in the key resources table.

This paper does not report original code.
Any additional information required to reanalyze the data reported in this paper is available from the lead contact upon request.

EXPERIMENTAL MODEL AND SUBJECT DETAILS

Mice

Five to six-week-old male C57BL/6JAusb mice from Australian BioResources were maintained under specific-pathogen-free conditions or germ-free conditions where specified. All experimental procedures involving animals were approved by the University of Sydney Animal Ethics Committee under protocol number 2014/696. Mice were housed individually with water and food (AIN93G; Specialty Feeds) access ad libitum. Experiments were repeated 4 times at the day 6 endpoint and 3 times at the day 3 endpoint.

HEK 293 cell lines

HEK-Blue^{TM} murine TLR4 and TLR2 reporter HEK 293 cell lines were maintained under standard cell culture conditions (37°C, 5% CO_2) in DMEM containing 10% (v/v) heat-inactivated fetal bovine serum, 10,000 U/mL penicillin, 10,000 μg/mL streptomycin, 100μg/mL Normocin and HEK-Blue^{TM} Selection (1:250 dilution).

METHOD DETAILS

Germ free mouse microbial recolonisation

Total cecal content from n = 6 mock or n = 6 IMQ-treated mice were pooled and resuspended in sterile PBS at a concentration of 100 mg/mL and homogenised. Suspensions were filtered through a 100 μm filter mesh, and 200 μL of this suspension were immediately administered intragastrically to germ-free mice. DNA was extracted from suspension to confirm comparable bacterial load was administered to recipient mice. Recolonisation was performed through a single oral administration of cecal content, and recipient mice were cohoused.

Imiquimod-induced psoriasis induction

Dorsal hair was shaved using clippers and depilatory cream (Nair). Psoriasis was induced by daily applications of 2mg imiquimod (42.6mg Aldara with 5% imiquimod w/w) for 3 or 6 days as previously described (van der Fits et al., 2009). Erythema and scaling were assessed daily and each given a score between 0 and 4: 0, none; 1, slight; 2, moderate; 3, marked; 4, very marked (van der Fits et al., 2009). Cumulative disease severity score was obtained by adding the erythema and scaling scores. Electronic callipers were used to measure skin thickness daily (van der Fits et al., 2009). Elizabethan collars were purchased from Able Scientific and placed on mice anesthetised with isoflurane from the day of initial imiquimod application onwards where indicated. Mice were checked regularly to ensure normal breathing and food/water intake. Mice were single-housed during all experiments involving imiquimod.

Administration of immune modifying particles (IMP)

Mice were given 4.26×10^9 particles of poly(lactic-co-glycolic acid) (PLGA) negatively charged, carboxylated IMP with a diameter of 500 nm (Phosphorex Inc, Hopkinton, MA, USA) via intravenous tail vein injection daily in 200ul sterile PBS, beginning at the time the imiquimod was administered. PBS alone was used for untreated mice.

DSS colitis model and scoring

Mice were treated with 3% dextran sulfate sodium (MP Biomedicals) in drinking water for 5 days. Mice were monitored and given a clinical score daily of 1–8, as previously described (Macia et al., 2015). Briefly as follows: 0: no sign of disease; 1: bloody stool and normal faeces; 2: bloody stool and soft faeces; 3, bloody stool and pasty faeces; 4: bloody stool and liquid faeces; 5: moderate rectal bleeding; 6: severe rectal bleeding; 7: haemorrhagia and 8, death. Colon length was measured at the experimental endpoint (day 5). Histology scoring was performed blinded on paraffin-embedded tissue stained with H and E, as previously described (Macia et al., 2015). Tissue damage and inflammatory infiltration scores (0 to 3 each) were added to give a histology score of 0 to 6.

BrdU staining for flow cytometry

Mice were given 1 mg of bromodeoxyuridine (BrdU, BD Biosciences kit number 552598) by intraperitoneal injection four hours before sacrifice, to analyse cell proliferation. A BD Biosciences kit was used to stain proliferating cells using BrdU-specific antibody conjugated to APC, according to manufacturer's instructions.

IL-17 administration

IL-17A/F recombinant protein (Biolegend) was injected intravenously with a dose of either 150 or 600pg in a total volume of 200μL saline daily for 3 days. Control mice received saline alone. Mice were sacrificed using CO_2 asphyxiation 24h after the final treatment and organs harvested for flow cytometry and qPCR.

Flow cytometry

Spleens and lymphoid organs were mechanically disrupted. The colon was washed in PBS, cut into small pieces and intraepithelial cells removed by incubating in HBSS solution containing 100 U/Ml penicillin-streptomycin (Sigma), 5% FCS, 15mM HEPES and 5mM EDTA for 40 minutes at 200 rpm, 37°C. Whole tissue was then digested in HBSS containing 100 U/Ml penicillin-streptomycin (Sigma), 10% FCS, 15mM HEPES +6.7mg/mL Collagenase type IV (GIBCO) for 40 minutes at 200 rpm, 37°C. After a brief vortex, the supernatant was pushed through a 70μm filter and isolated using 40% and 80% Percoll gradient. Lamina propria leukocytes were isolated from the middle ring of the Percoll gradient, washed and pelleted in complete media (RPMI+ 100 U/mL penicillin-streptomycin (Sigma), 10% FBS, 2mM L-Glutamine (Sigma) and 0.01M HEPES (Thermo Fisher Scientific). Dissociated cells were first incubated with FcR blocker (Biolegend) and Live/dead stain (ThermoFisher) in PBS for 30 minutes on ice. For intracellular cytokine staining, cells were stimulated with phorbol 12-myristate 13-acetate (PMA), ionomycin and brefeldin A in complete media for 4 hours. After surface staining, cells were fixed and stained using a BD Cytofix/Cytoperm kit (BD Biosciences) as per manufacturer's instructions. Antibodies used is listed in the key sources table. Data was acquired using a BD LSR II (5-laser) flow cytometer and analysed using FlowJo software. Automatic compensation was performed on the flow cytometer before running samples.

Histology and dermal measurements

Paraffin-embedded skin samples were sectioned and stained with haematoxylin and eosin. Slides were visualised using light microscopy (Zeiss Axioscope) and ImageJ (NIH) used for measuring dermal thickness. A minimum of 4 fields of view at 10x magnification were taken per mouse and 20 measurements per field.

Bacteria 16S rRNA gene amplicon sequencing and bioinformatics

DNA from fecal samples were extracted using the FastDNA Spin Kit for Feces (MP Biomedicals) following the manufacturer's protocol. 16S rRNA DNA was sequenced commercially (Ramaciotti Centre for Genomics, The University of New South Wales) on an Illumina Miseq (2 × 250bp) targeting the V4 region (515f-806r). Amplicon sequence variant (ASV) was generated using the DADA2 pipeline (Callahan et al., 2016) using R software (3.6.1) and taxonomy was assigned using the Ribosomal Database Project naive Bayesian classifier with species level taxonomy assignment (Callahan, 2017). ASVs that occurred below 0.01% of total abundance were removed. Zero replacement of ASV was achieved by scaling ASVs with a pseudocount of 1 and data was then center log-ratio (CLR) transformed, which is required for the analysis of compositional dataset (Gloor et al., 2017). Differences in microbiome composition between groups was determined by PERMANOVA test of Aitchison distance matrix (Euclidean distance of CLR transformed data), after validation of homogeneity of variances by betadisper testing (vegan 2.5–6). Differentially abundant taxa were determined by ALDEx2 (1.20.0) and taxa was considered differentially abundant when Benjamini-Hochberg-corrected expected p-value for both Welch's t test and Wilcoxon test were <0.05. Metagenomic prediction from ASV data was performed using the PICRUSt2 pipeline, using default parameters and differential analysis performed with ALDEx2 as above. For Spearman's correlation between taxa and experimental variables, taxa data were first transformed using the Hellinger method and correlation was performed using R software. Sequencing data were deposited in the European Nucleotide Archive under accession number PRJEB47653.

For RNA-seq analysis, sequencing data was downloaded from Gene Expression Omnibus from previous study (GEO: GSE150851) (Chang et al., 2021). Data was analyzed with the Gene Set Enrichment Analysis (GSEA) software based on the developer's protocol (Subramanian et al., 2005).

Bacterial metabolite analysis using nuclear magnetic resonance (NMR) spectroscopy

Quantitative measurements of metabolites in caecum contents were determined by nuclear magnetic resonance (NMR) spectroscopy. Briefly, caecum contents were homogenized in deuterium oxide, the homogenate was filtered through a 3 kDa membrane and then metabolites in the filtrate were extracted from the aqueous phase of a deuterium methanol/deuterium chloroform mixture. The samples, containing 4,4-dimethyl-4-silapentane-1-sulfonic acid as an internal standard, were analyzed on a Bruker 600 MHz NMR data is normalised per mg of caecal content.

RNA extraction and real Time PCR

Skin samples were snap-frozen in liquid nitrogen and stored in −80°C until analysis. Samples were homogenised with a Qiagen TissueLyser LT in TRI Reagent and a metal bead to extract RNA according to manufacturer's instructions (Sigma-Aldrich). RNA was converted into cDNA using iScript RT Supermix (BioRad) according to manufacturer's instructions. qPCR was performed on a LightCycler 480 (Roche) using SYBR Green (Biorad). The sequences of primers are listed in the key resources table.

Colon *ex vivo* cell culture

Colonic lamina propria cells were isolated as indicated above for flow cytometry. Cells were then counted using trypan blue and placed into 24-well tissue culture plates (corning) at a density of 1 million per well in 2mL complete media (DMEM +100 U/mL penicillin-streptomycin (Sigma), 10% FBS, 2mM L-Glutamine (Sigma) and 0.01M HEPES (Sigma) +/− sodium succinate (500μM) (sigma) as indicated. Cells were incubated at atmospheric or 3% O_2 as indicated and 5% CO_2. Cells were stained for flow cytometry after 72h in culture.

QUANTIFICATION AND STATISTICAL ANALYSIS

Statistics

Statistics were performed using Prism GraphPad. Normal distribution within sample groups was first determined using the D'Agostino & Pearson normality test. Subsequently, non-parametric Kruskal-Wallis test (non-normal distribution) or parametric one-way ANOVA (normal distribution) statistical analysis was utilised when comparing three or more groups with one independent variable. A non-parametric Mann Whitney U -test (non-normal distribution) was utilised when comparing two groups. Two-way ANOVA was used when comparing more than 2 groups and/or more than two independent variables, such as time and treatment. $p < 0.05$ was considered statistically significant.